1   **Title: Mammalian resilience to megafire in western U.S. woodland savannas**

2

3   **Authors: Kendall L. Calhoun[1], Benjamin R. Goldstein[1], Kaitlyn M. Gaynor[1,2], Alex**

4   **McInturff[1,3], Leonel Solorio[1], Justin S. Brashares[1]**

5

6   [1]Department of Environmental, Science, Policy, and Management, University of California

7   Berkeley, 137 Mulford #3114, Berkeley, CA, 94720, USA

8   [2] Departments of Zoology & Botany, University of British Columbia, BC, Canada V6T 1Z4

9   [3]School of Environmental and Forest Sciences, University of Washington, Anderson Hall, Box

10   352100, Seattle, WA, 98195, USA

11

12   *Corresponding Author: kendallcalhoun@berkeley.edu, 210 Wellman Hall, Berkeley, CA,

13   94720, USA

14

15

16

17

18

19

20

21

22

23

24   **Abstract**

25   Increasingly frequent megafires, wildfires that exceed the size and severity of historical fires, are

26   dramatically altering landscapes and critical habitats across the world. Across the western U.S.,

27   megafires have become an almost annual occurrence, but the implications of these fires for the

28   conservation of native wildlife remains relatively unknown. Woodland savannas are among the

29   world's most biodiverse ecosystems and provide important food and structural resources to a

30   variety of wildlife, but they are threatened by megafires. Despite this, the great majority of fire

31   impact studies have only been conducted in coniferous forests. Understanding the resistance and

32   resilience in wildlife assemblages following these extreme perturbations can help inform future

33   management interventions that limit biodiversity loss due to megafire. We assessed the resilience

34   of a woodland savanna mammal community to the short-term impacts of megafire using a

35   before-after-control comparison. Specifically, we utilized a 5-year camera trap data set (2016-

36   2020) from the Hopland Research and Extension Center to examine the impacts of the 2018

37   Mendocino Complex Fire, California's largest recorded wildfire at the time, on the distributions

38   of 12 observed mammal species. We used single species occupancy models to quantify the effect

39   of megafire on species' space use and a multi-species occupancy model for robust estimates of

40   fire's impacts on species diversity across space and time. Megafire had a strong, negative effect

41   on mammalian occupancy and activity directly following wildfire, but most species showed high

42   resiliency and returned to were resilient and returned to activity and occupancy levels

43   comparable to unburned sites by the end of the study period. Following fire, species richness was

44   highest in burned areas which retained some canopy cover. Change in habitat use following

45   wildfire varied by species: several species temporarily reduced their use of severely burned

46   areas, while others became more active in those areas. Fire management that prevents large scale

2

47   canopy loss is critical to providing refugia for vulnerable species immediately following fire in

48   oak woodlands, and likely other mixed-forest landscapes.

49

50   Key words: megafire, camera trap, occupancy, California, oak woodland, resilience, resistance,

51   richness

52

53

54

55

56

57

58

59

60

61

62

63

64

65

66

67

68

69

1. Introduction

In an era of unprecedented global change, 21st century megafires present an intensifying threat to critical habitat and wildlife species in fire-prone ecosystems around the world (Nimmo et al., 2021). Megafires, here defined as wildfires that are larger and more severe than historic wildfires, drive dramatic and lasting changes to whole ecosystems (Stephens et al., 2014). These far-reaching environmental shocks can quickly homogenize landscapes and present short- and long-term challenges for wild animal species (Adams, 2013; Steel et al., 2021). As megafires continue to increase in frequency and scale, the gap in our understanding of how wildlife species respond and recover to megafire events becomes more glaring (Jolly et al., 2022). Such information is essential to the conservation of fire-prone landscapes and the formation of management strategies that bolster resilience to severe wildfire. Like other regions of the world, California, and the western U.S. generally, have experienced its largest and most severe fires in the last 20 years (Li & Banerjee, 2021). With a diverse range of ecosystems, and as a global hotspot in biodiversity, California presents an important opportunity to understand the impacts of megafire on diverse ecological communities and to observe how patterns of species vulnerability or resilience may interact with these perturbations.

To address the challenges presented by megafire and other disturbances, contemporary conservation often emphasizes building resistance and resilience to better protect ecosystems from future change (Miller et al. 2021, Heller & Zavaleta, 2008). Resilience, the ability of a community or population to recover to baseline conditions following disturbance (Holling, 1973), and resistance, the degree to which an ecosystem property, or population, changes directly following a disturbance (Pimm 1984), are key elements that interact to maintain ecological

4

93   integrity following disturbance. Though resilience is a useful theoretical concept, it is often

94   difficult to implement due to the challenges of characterizing and quantifying it (Standish et al.

95   2014; Ingrishch and Bahn, 2018). Application is made more difficult by the rarity and dynamic

96   nature of baseline ecological information to compare against recent change (Soga & Gaston,

97   2018; Cammen et al., 2019). A deeper understanding of context-specific resilience and resistance

98   to disturbance is needed at multiple ecological scales (organismal, species, community, and

99   ecosystem) to predict, prevent, and combat the effects of global change.

100

101   At the scale of species, resilience and resistance to wildfire will be governed, in large

102   part, by species' traits (e.g., home range size, diet, trophic level) (Jager et al. 2021). For example,

103   body size is a key trait that determines how species interact with their environment by dictating

104   how they interact with other species (e.g., diet and competition) and how they are able to

105   navigate space. Previous work has shown that body is closely correlated with home range size

106   for mammal species (Reiss 1984). Home range size may directly impact the ability of

107   populations to cope with expansive disturbances like megafire. Species with larger home ranges

108   or without specific habitat requirements (e.g., generalists and opportunists) may be better

109   equipped to adapt to the sudden shifts caused by megafire (Nimmo et al., 2019; Geary et al.

110   2020).

111

112   Characteristics of a wildfire itself, such as severity, heterogeneity, and burn patch size,

113   may also interact with species traits to determine species-specific responses to wildfire. Fire

114   severity, specifically the measure of change in above and below ground biomass as a result of

115   fire, is thought to be an important characteristic of fire regimes that directly impacts wildlife

116   (Keeley, 2009). By altering available food resources, megafire may change the distribution of

117   wildlife species in recently burned landscapes (Cherry et al., 2018). Changes to the structure of

118   the physical landscape may also alter how species are able to navigate habitats (Kreling et al.

119   2021). These changes, in turn, may reshape species interactions, such as predation (Jennings et

120   al. 2016). Both mechanisms – changes to resource availability and physical habitat – may

121   influence the distribution of wildlife species following extreme fire events, but the context in

122   which they do may be species and fire dependent (Geary et al., 2020).

123

124   In this study, we explored the influence of fire occurrence and canopy cover on the

125   distribution of oak woodland mammal species over time by taking advantage of an opportunistic

126   natural experiment. We assessed the impacts of the Mendocino Complex Fire, one of the largest

127   fires in recorded California history, on the occupancy of 12 mammal species at the University of

128   California Hopland Research and Extension Center (hereafter HREC) in northern California. We

129   apply the concepts of resilience and resistance at the population and community scales to observe

130   how wildlife species respond to megafire. By using camera trap data collected before, during,

131   and after the fire, along with an occupancy modeling framework (Mackenzie et al., 2002), we

132   had the rare opportunity to assess how animal activity patterns, habitat usage, and patterns of

133   diversity changed and recovered over time. For the purposes of our study, we deemed species

134   "resilient" if the species' single-species occupancy model estimated no effect of burn history on

135   intensity of use or occupancy in the lag years following fire, or if we observed an increase in

136   these estimates relative to unburned sites. We deemed species "resistant" to fire if the species'

137   single-species occupancy model estimated no effect of the burn on intensity of use or occupancy,

138   or if either of these estimates increased relative to unburned sites during the year of the fire.

139   In assessing species-level responses to megafire in our system, we predicted that larger-

140   bodied species would be less likely to alter their activity and occupancy within burned areas or

141   areas with low canopy cover due to their increased vagility (high resistance and resilience). We

142   predicted that species richness would decrease in recently burned areas and slowly return to pre-

143   burned conditions over time associated with canopy recovery. Detailing the capacity of these

144   species to recover is vital to inform better conservation decisions for woodland mammal

145   communities by 1) identifying vulnerable species that may need to be prioritized in post-fire

146   recovery management, and 2) identifying landscape features that may enhance the resilience and

147   resistance of mammal communities to megafire.

148

149   **2.   Materials and Methods**

150   2.1 Study Area and Fire History

151   We conducted our study at the 5,300 acre U.C. Hopland Research and Extension Center (HREC)

152   in Mendocino County, northern California (39°00′ N, 123°04' W). The HREC ecosystem is

153   composed of a diverse range of habitat types including grassland, oak woodland, and shrubland

154   (chaparral). HREC is situated at an intersection of wildlands and ranchlands; it provides habitat

155   for a diverse group of wildlife and serves as pastoral land for people and livestock. The region is

156   characterized by a Mediterranean climate, with mild seasons and rains in the winter.

157

158   On July 27, 2018, the 2018 River Fire, part of the much larger 2018 Mendocino Complex

159   Fire, burned over 3,400 acres of the 5,300 acre Hopland Research and Extension Center (Figure

160   1, Appendix S1 – Figure S1.1). At the time, the Mendocino Complex Fire was the largest fire in

161   California's recorded history, burning 459,123 acres. The scale and severity of this fire

162   contrasted the historical fire regime in this region which is characterized by frequent, cooler fires

163   in woodlands and infrequent, more severe burns in shrubland habitats (Syphard and Keeley,

164   2020).

165

166   2.2 Camera Survey and Study Species

167   We established a grid of 36 motion-sensor trail cameras (Reconyx Hyperfire HC600), and, for

168   this study, extracted photos taken from March 2016 to December 2020. We placed cameras at

169   the centroid of hexagonal grid cells, where each camera was positioned 750 m apart from its six

170   neighbors. At each grid cell center, we placed a camera at the most suitable location (e.g., game

171   trails) within 50 m of the centroid to maximize detection probability of species 1m above the

172   ground. We programmed cameras to take 3 photos per trigger. Of the 36 total cameras, 25 were

173   within the fire perimeter of the 2018 River Fire. Seven of these cameras were not operational

174   following the fire and were replaced when conditions were safe to do so in August 2018. For this

175   reason, and due to a natural increase in biodiversity detected in the fall months due to concurrent

176   acorn masting, we restrict our sampling window for analyses to October 1st - November 30th for

177   each year.

178

179   The species in all collected images were classified by two independent observers who

180   were members of the Brashares Lab at the University of California - Berkeley. We created

181   species record tables for each year from these cataloged images using the 'camtrapR' package in

182   R (Niedballa et al., 2016; Team, R. C, 2020). To create independent detections for analyses, we

183   aggregated images of the same species and site using a 15-minute quiet period.

184

185   For this study, we modeled occupancy for the 12 mammal species with 10 or more

186   independent detections across the entire study period: black bear (*Ursus americanus*), bobcat

187   (*Lynx rufus*), coyote (*Canis latrans*), black-tailed deer (*Odocoileus hemionus columbianus*), gray

188   fox (*Urocyon cinereoargenteus*), western gray squirrel (*Sciurus griseus*), California ground

189   squirrel (*Otospermophilus beecheyi*), black-tailed jackrabbit (*Lepus californicus*), mountain lion

190   (*Puma concolor*), wild boar (*Sus scrofa*), raccoon *(Procyon lotor*), and striped skunk (*Mephitis*

191   *mephitis*).

192

193   2.3 Environmental Covariates

194   We predicted that canopy cover, time since burn, elevation, and landscape ruggedness would be

195   associated with occupancy and animal activity across our species assemblage. Independent of

196   fire, elevation and ruggedness are important factors in shaping mammal habitat selection in

197   similar ecosystems (Poley et al., 2014; Furnas et al. 2021). Canopy cover is also an important

198   predictor of mammal habitat use (Allen et al. 2015; Bose et al., 2018) and canopy cover loss

199   following fire serves as an important proxy for fire severity in the burned areas of our study site.

200   Finally, time since burn was included because certain species may preferentially occupy or avoid

201   burned areas depending on how much time has passed since the area burned (Gonzalez et al.,

202   2021).

203

204   We obtained elevation data for each site using the ASTER Global Digital Elevation

205   Model (NASA and METI 2011) and extracted elevation values at each camera site. We then

206   calculated ruggedness, the variability in slope and aspect within a neighborhood of 2,500 m^2,

207   using the Vector Ruggedness Measure tool for ArcGIS around each camera site (Hobson, 1972).

208

209   We estimated canopy cover using 20-meter resolution imagery from Sentinel hub

210   (Sentinel Hub, 2021) to create canopy rasters via object-based image analysis and supervised

211   classification in ArcGIS Pro (ESRI, 2011) for each year (2016-2020). These rasters were visually

212   verified using fine scale, 3-m resolution imagery via Planet Labs (Tilahun & Teferie, 2015;

213   Planet Team, 2017; Sunde et al., 2020). A full description of methods used to create and verify

214   canopy rasters can be found within Appendix S2 (Appendix S2 – Figure S2.1; Appendix S2 –

215   Figure S2.2). Canopy cover values were extracted from a 100m buffer around each camera site

216   for each year to calculate percent canopy cover within the buffered radius.

217

218   Lastly, we created a "time since burn" categorical variable that varied by site and year to

219   describe whether a camera site was unburned (Unburned), burned that year (Burned - 2018),

220   burned > 1 year ago (Burn Lag1 - 2019), or burned > 2 years ago (Burned Lag2 - 2020)

221   (Appendix S4).

222

223   We predicted that Julian day, Julian day squared, time since burn, and the presence of

224   microsite attractants (roads and water troughs) would directly affect the detectability of species

225   across sites and observation periods. Species activity has been shown to be correlated closely

226   with seasonality (Kays et al., 2020), and we included Julian day and Julian day squared to

227   account for seasonal differences throughout the study. Roads and water troughs have also been

228   shown to strongly attract usage by various species (Rich et al. 2019; Hill et al., 2021). To

229   account for these features in our study, we created a site-level "microsite attractant" binary

230   categorical variable that indicated whether a camera was pointed towards the attractants present

231   in our study, roads or water troughs.

232

233   2.4 Occupancy Modeling Framework

234   For each species, we fit a hierarchical single-species occupancy model (SSOM) to estimate

235   relationships between covariates and within- and between-site variation (MacKenzie et al.,

236   2002).

237   The single-species occupancy model for each species was defined by the following

238   equations:

239

240    $\text{logit}(\psi_{i,t}) = A0 + A1 \times \text{Ruggedness}_i + A2 \times \text{Elevation}_j + A3 \times \text{Canopy}_{i,t} +$

241            $A4 \times \text{Burn History Category}_{i,t} + A5 \times \text{Canopy}_{i,t} \times \text{Burn History Category}_{i,t} +$

242            $\text{Site Random Effect}_i$

243

244    $\text{logit}(p_{i,j,t}) = B0 + B1 \times \text{Attractant}_i + B2 \times \text{Julian Day}_{i,j,t} +$

245            $B3 \times \text{Julian Day}^2_{i,j,t} + B4 \times \text{Burn History Category}_{j,t}$

246

247    $z_{i,t} \sim \text{Bernoulli}(\psi_{i,t})$

248    $y_{i,j} \sim \text{Bernoulli}(p_{i,j,t} z_{i,t})$

249    $\text{Site Random Effect}_i \sim \text{Normal}(0, \sigma)$

250

251   In the above equations occupancy, $\psi_{i,t}$ is the probability that at least one individual of a

252   given species is present at site i, year t during a sampling period (one site in one season), and $p_{i,j,t}$

253   is the probability of detecting an individual a that site given that the site is occupied (i.e. $z_i = 1$)

254   (Burton et al., 2015). In this model, $p_{i,j}$ incorporates variation due to both. We treated each

255   camera in each year as a unit of closure, assuming a shared underlying occupancy state, and

256   considered each sampling week a replicate observation. These values are logit-linked to a linear

257   combination of covariates. We included a site random effect on occupancy probability to account

258   for non-independence between surveys at sites, a design choice sometimes referred to as a

259   "stacked" model.

260

261   Alongside the single-species occupancy models, we also fit an additional multi-species

262   occupancy model (MSOM) to investigate the effects of megafire on community richness and

263   diversity (Appendix S2). The MSOM is defined equivalently to the single-species model with the

264   addition of a hyperparameter relationship stating that each species-specific covariate effect is

265   drawn from a shared normal distribution. This species random effect/hyperparameter approach

266   shrinks species-specific coefficients toward their community means and gives more robust

267   inference on community-level variables (Iknayan et al., 2014; Devarajan et al., 2020). Using this

268   MSOM, we derived species richness estimates at each camera site. In order to assess the effects

269   of fire on species composition, or beta diversity, we also derived Hill number estimates based on

270   occupancy probabilities to evaluate the effect of wildfire on community composition across sites

271   (Gaynor et al. 2020, Broms et al. 2014). The first Hill number estimate represented Shannon

272   diversity and the second Hill Number represented Simpson diversity. We interpret the

273   community hyperparameters and estimated diversity metrics from the MSOM, alongside species-

274   specific estimates obtained from each SSOM.

275

276   Across both model types, we used weakly informative priors: all linear covariate priors or

277   linear covariate hyperparameter means were set to N(0, sd = 2.5) and all random effect and

278   hyperparameter standard deviation priors were half-Cauchy with scale parameter 2.5 (Northrop

279   and Gerber 2018). We implemented both SSOMs and the MSOM and estimated them with

280   Markov chain Monte Carlo (MCMC) using the R packages NIMBLE and nimbleEcology (de

281   Valpine et al., 2017; Goldstein et al., 2020).

282

283   All continuous covariates were standardized to have a mean of 0 and standard deviation

284   of 1. We also checked for collinearity between each covariate to ensure multi-collinearity would

285   not confound analyses (collinearity cut-off at r > 0.7) (Dormann et al., 2012). In addition to site-

286   level covariates on occupancy probability (ruggedness, elevation, canopy) and the observation-

287   level covariates on detection (Julian date, Julian date square, presence of attractant), we included

288   the fixed effect of "time since burn" in both submodels. In the occupancy submodel, we also

289   included an interaction term between canopy cover and time since burn (canopy cover x time

290   since burn). We used Watanabe-Akaike information criterion (WAIC) to compare and select the

291   burn history parameterization as shown in Appendix S4 (Appendix S4 – Table S4.1) (Gelman et

292   a., 2014).

293

294   Several species in this study are wide-ranging, with home ranges that may contain more

295   than one camera trap station (Neilson et al., 2018). Therefore, we interpret occupancy, Ψ, as "site

296   use" instead of true occupancy (Kays et al., 2020). Previous work has shown that detection

297   probability, p, is correlated with local species abundances (Royle 2004, Royle & Nichols, 2003)

298   and/or changes in behavior to avoid perceived risk (Suraci et al. 2021). We therefore interpret

13

299   detection probability as each species' intensity of use of occupied sites (hereafter referred to as

300   intensity of use) to observe how wildfire may influence species activity at burned sites.

301

302   2.6 Assessing Model Convergence & Fit

303   We ran each SSOM for 15,000 iterations, with a 500 iteration burn in across 2 chains. We ran the

304   MSOM for 10,000 iterations, with a burn in of 1,000 iterations across 2 chains. These values

305   were chosen via use of the Gelman-Rubin diagnostic–we ensured that all parameters had $\hat{r}$

306   values of <1.1 (Gelman et al., 2004). Parameter chains were visually assessed for convergence.

307

308   For each single-species model, we simulated a new dataset using the parameters in each

309   MCMC sampling iteration. We calculated the deviance of each of these datasets, yielding a

310   posterior distribution of deviances produced from data simulated under the true model. We

311   compared observed model deviances to this posterior to check for evidence that the data do not

312   correspond to the fit model (Gelman et al. 1996, MacKenzie et al., 2017). Finally, within each

313   model, we assessed a covariate as being a significant predictor of occupancy or intensity of use if

314   the 90% credible interval for that variable did not overlap zero. We use this definition to describe

315   significance under Bayesian inference in the following cases.

316

317   **3. Results**

318   3.1 Camera Trap Survey Results

319   We observed 12,532 detections of the 12 mammal species of interest during our study period

320   across a total of 10,427 trap nights. Black-tailed deer were the most detected species (n = 9,905),

321   while mountain lions were photographed least often (n = 16) (Appendix S1 - Table S1.4).

322

3.2 Species-level Responses to Wildfire

For all twelve species, posterior predictive checks indicated goodness of fit within acceptable

bounds. The observed deviance in all models did not differ from the posterior distribution of

simulated deviances (Appendix S1 - Fig. S1.2).

327

3.2.1 Predictors of Intensity of Use

Intensity of use at camera trap sites was strongly associated with the presence of microsite

attractants near cameras (roads or water troughs) across all study species except ground squirrel

and wild boar (Appendix S1 - Figure S1.3). Julian day and Julian day squared, representing

seasonality, were strong predictors of activity for several species as well, including black-tailed

deer, western gray squirrel, striped skunk, and wild boar (Appendix S1 - Figure S1.3).

334

Overall, wildlife activity within the burned areas decreased (90% CI did not overlap zero)

for five of the examined species (black bear, black-tailed deer, western gray squirrel, California

ground squirrel, and raccoon) and may indicate an initial vulnerability, or low resistance, to

wildfire across these species (Figure 3). Originally, we anticipated that cleared vegetation caused

by recent wildfires may increase the detectability of species on cameras, but the observed results

dispute this. Coyotes were the only species to increase their intensity of use of burned areas

during this time period. Intensity of use of burned areas changed over time for certain species.

For example, black bear activity was greater two years following the fire (Burn Lag2) in burned

areas relative to unburned areas (Fig 3).

344

345   3.2.2 Predictors of Occupancy

346   Landscape ruggedness was strongly correlated with an increase in occupancy for two carnivore

347   species (coyote and bobcat) (Appendix S1 - Figure S1.4). Similarly, elevation was a predictor of

348   occupancy for the two largest carnivores (black bear and mountain lion), with higher occupancy

349   at higher elevations (Appendix S1 - Figure S1.4). Irrespective of time since burn, canopy cover

350   was strongly and positively correlated with occupancy of mountain lions.

351

352   The effect of time since burn on occupancy was species-specific and changed across

353   time. For example, jackrabbits were more likely to occupy burned sites two years post-fire

354   (2020) relative to unburned camera sites, but not during the year of the fire (2018) or the

355   following year (2019) (Appendix S1 - Figure S1.4). In contrast, gray fox and wild boar were

356   more likely to occupy burned sites one-year post-fire (2019), but only sites that maintained high

357   canopy cover and not during the year of the fire (2018) or 2 years post-fire (2020) (Appendix S1

358   - Figure S1.4).

359

360   3.3 Community-level Responses to Wildfire

361   Within recently burned sites (immediately following fire in Fall 2018), species richness was

362   significantly higher at sites with higher canopy cover (mean = 6.31, 90% CI: 4.99 – 7.75) relative

363   to sites with unburned canopy (Fig 4). This effect decreased over time, with richness two years

364   post-burn (Burn Lag2) being most comparable to richness estimates at unburned sites. Species

365   richness was not notably different at each of the recently burned areas relative to unburned

366   camera sites (Figure 4, Appendix S1 – Figure S1.4, Appendix S1 – Figure S1.5, Appendix S1).

367

368   We found that Shannon diversity (community composition evenness), represented by the

369   first Hill number, was not significantly different between burn lag periods. Similarly, Simpson

370   diversity (community composition dominance), represented by the second Hill number, did not

371   differ between burn lag periods, but was slightly higher at recently burned sites and burn sites

372   one year following fire (Burn Lag 1) with high surviving canopy cover (Appendix S1 – Figure

373   S1.6).

374

375   **4. Discussion**

376   Patterns of wildlife occupancy, intensity of use, and species richness changed following a

377   megafire in a northern California oak woodland. Intensity of use by larger mammals at burned

378   sites decreased during the year of the fire as well as for the two following years. A few select

379   species (e.g., coyotes and gray foxes) increased their occupancy and/or intensity of use at burned

380   sites, potentially taking advantage of burned areas with a decreased presence of larger predators

381   or increased exposure of prey species. Despite the observed short-term changes in wildlife

382   intensity of use, most species appear to be resilient to the impacts of wildfire given that they

383   returned to pre-fire intensity of use and occupancy within the two years following the fire. We

384   estimated that species richness increased at burned sites during the year of the fire relative to

385   unburned sites, but only at sites that burned at low severity and maintained high canopy cover.

386   These sites of higher canopy cover may act as temporary refugia for several species amidst a

387   severely burned landscape.

388

389   Species for which canopy cover was estimated to be a significant positive predictor of

390   occupancy were deemed as having "low resistance" due to severe fire likely removing

17

391   considerable canopy cover in the short-term. The resilience of canopy-sensitive species (e.g.,

392   mountain lions and gray squirrels) likely depends on the ability of burned areas to naturally

393   regenerate over time. Although we observed an initial decrease in wildlife intensity of use in

394   recently burned areas, we found that most species appeared to be resilient to the effects of

395   wildfire (10 of the 12 examined species) (Table 1). By the end of our study, two years post-fire,

396   we found that the occupancy and intensity of use of most species was equal to or greater than

397   that of unburned sites. In addition, species richness and beta diversity (represented by the Hill

398   Numbers) at burned sites was comparable to unburned sites by the end of the study, suggesting

399   that community structure and composition were also resilient to megafire on these time scales.

400

401   We found little evidence to support our initial hypothesis that greater body size increases

402   the likelihood of a species being resistant or resilient to wildfire. Contrary to our initial

403   hypotheses, some smaller species appeared to increase their occupancy of areas following

404   wildfire (e.g., black-tailed jackrabbits) and several larger-bodied species decreased their intensity

405   of use of recently burned areas (e.g., black bears and black-tailed deer). However, of the five

406   species that displayed low resistance to wildfire, only the two smallest-bodied species (western

407   gray squirrel and raccoon) did not have intensity of use and/or occupancy levels that were

408   comparable to unburned conditions by the end of the study. Thus, body-size may play some

409   smaller role in mediating longer-term resilience to wildfire disturbance for more vulnerable

410   species. For larger, more mobile species, like black-tailed deer and black bears, changes in

411   intensity of use may actually represent shifts in activity centers, alterations in movement paths,

412   or avoidance of burned areas altogether following wildfire (Jager et al., 2021). As severe fire

413   modifies the structure of vegetation, animals may adjust their navigation of landscapes to

414　minimize risk and maximize access to remaining resources (Nimmo et al., 2019; Geary et al.

415　2020; Kreling et al. 2021). This behavioral response may grant these larger-bodied species some

416　level of adaptive capacity to quickly leave areas that are recently burned and return when

417　conditions are more favorable.

418

419　　　　Areas that recently burned that also maintained high canopy cover had an increase in

420　observed species richness relative to unburned sites and sites post-fire (2019 and 2020)

421　suggesting that these sites may provide refugia for additional species directly following fire.

422　These canopied "islands" may provide important resources (forage and cover) that are lacking in

423　other parts of the recently burned landscape. Using pre-emptive prescribed burning and land

424　modification tools that prevent large contiguous megafire burns could help ensure patches of

425　refugia remain following fire. This may be one of the best strategies to enhance the long-term

426　resilience of these ecological communities from global change disturbances like megafire

427　(McWethy et al., 2019; Miller et al., 2021). This attractant effect towards canopied areas post-

428　megafire is apparent the year of the fire and decreases in the years following. Therefore, refugia

429　following megafire may be most critical in the immediate months following wildfire to ensure

430　species have access to resources before vegetation is able to recover naturally.

431

432　　　　Given our relatively small sample sizes, we did not explicitly model the effects of

433　wildfire on species interactions, but the results of the single-species occupancy models suggest

434　that interspecies interactions may contribute to the species-specific responses we observed.

435　While larger carnivores (e.g., mountain lion and black bear) decreased their occupancy and

436　intensity of use in burned areas, we observed that several medium-sized species increased their

437   activity (e.g., coyotes) and occupancy (e.g., gray fox and wild boar) of burned areas. These

438   results mirror the response of mesopredators to wildfire observed in similar studies within

439   California (Schuette et al., 2014; Jennings et al., 2016; Furnas et al., 2021). Predation mode may

440   also modify how certain predators respond to severe fire in woodlands. Loss in canopy cover

441   may reduce hunting success for ambush predators (e.g., mountain lions and bobcats) and increase

442   the hunting success of predators that favor more open areas (e.g., coyotes) across recently burned

443   woodlands (Benson et al, 2016, Doherty et al. 2022).

444

445   The increase in occupancy and intensity of use of mesopredators following fire may also

446   be an indirect response to the temporary removal or decreased presence of larger predators

447   within the system, as observed in other studies (Estes et al., 2011). Previous work shows that a

448   variety of global change pressures can trigger this "rewiring" of species composition and trophic

449   webs (Bartley et al., 2018, Suracci et al., 2021). Megafire could, at least temporarily, intensify

450   this effect, and exacerbate existing stressors on large carnivores, especially as the frequency,

451   size, and severity of megafires continues to increase. More research is necessary to examine the

452   impacts of megafire on these larger predators over a broader spatial and temporal context to

453   explicitly examine how and for how long these effects may alter species interactions, such as

454   predation (Doherty et al., 2022) and interspecies competition (Gigliotti et al., 2021).

455

456   Changes in historic fire regimes may pose a greater threat to woodland savanna

457   ecosystems and their wildlife communities relative to other ecosystem types worldwide (Kelly et

458   al. 2020, Calhoun et al., 2021). Due to the key services and habitat they provide around the world

459   (Veldman et al., 2015; Eastburn et al., 2017), it is essential that we prioritize developing effective

460   fire management tools for woodland savannas to protect their long-term ecological integrity

461   against shifting fire regimes. Our study highlights the vulnerability, resistance, and resilience of

462   certain woodland savanna wildlife species to megafire in the short-term, but more work is

463   needed to understand how these initial responses translate over longer time periods as structural

464   cover and vegetative food availability continue to change.

465

466   **5. Conclusion**

467   Frequent megafires have the potential to alter wildlife communities in fire-prone

468   ecosystems around the world. We found evidence of resilience to megafire in a woodland

469   savanna mammal community, potentially made possible by the availability of refugia following

470   megafire. These findings further corroborate the importance of spatial burn patchiness in mixed-

471   severity fire regimes, specifically from the perspective of wildlife. In woodland ecosystems,

472   management that can 1) prevent megafire or 2) facilitate the creation of more heterogeneous

473   landscapes following megafire may be the best strategies to enhance the resilience of mammal

474   communities to future megafires.

475

476

477

478

479

480

481

482

503

504

505

Literature Cited

Adams, M. A. (2013). Mega-fires, tipping points and ecosystem services: Managing forests and
  woodlands in an uncertain future. Forest Ecology and Management, 294, 250–261.
  https://doi.org/10.1016/j.foreco.2012.11.039

Allen, M. L., Elbroch, L. M., Casady, D. S., & Wittmer, H. U. (2015). Feeding and spatial
  ecology of mountain lions in the Mendocino National Forest, California. *California Fish
  and Game*, *101*(1), 51-65.

Bartley, T. J., McCann, K. S., Bieg, C., Cazelles, K., Granados, M., Guzzo, M. M., MacDougall,
  A. S., Tunney, T. D., & McMeans, B. C. (2019). Food web rewiring in a changing world.
  Nature Ecology & Evolution, 3(3), 345–354. https://doi.org/10.1038/s41559-018-0772-3

Bose, S., Forrester, T. D., Casady, D. S., & Wittmer, H. U. (2018). Effect of activity states on
  habitat selection by black-tailed deer: Activity States and Habitat Selection. The Journal
  of Wildlife Management, 82(8), 1711–1724. https://doi.org/10.1002/jwmg.21529

Broms, K. M., Hooten, M. B., & Fitzpatrick, R. M. (2015). Accounting for imperfect detection in
  Hill numbers for biodiversity studies. Methods in Ecology and Evolution, 6(1), 99–108.
  https://doi.org/10.1111/2041-210X.12296

Burton, A. C., Neilson, E., Moreira, D., Ladle, A., Steenweg, R., Fisher, J. T., Bayne, E., &
  Boutin, S. (2015). REVIEW: Wildlife camera trapping: a review and recommendations
  for linking surveys to ecological processes. Journal of Applied Ecology, 52(3), 675–685.
  https://doi.org/10.1111/1365-2664.12432

Calhoun, K. L., Chapman, M., Tubbesing, C., McInturff, A., Gaynor, K. M., Van Scoyoc, A.,
  Wilkinson, C. E., Parker-Shames, P., Kurz, D., & Brashares, J. (2021). Spatial overlap of

528   wildfire and biodiversity in California highlights gap in non-conifer fire research and

529   management. Diversity and Distributions, ddi.13394. https://doi.org/10.1111/ddi.13394

530   Cammen, K. M., Rasher, D. B., & Steneck, R. S. (2019). Predator recovery, shifting baselines,

531   and the adaptive management challenges they create. Ecosphere, 10(2).

532   https://doi.org/10.1002/ecs2.2579

533   Cherry, M. J., Chandler, R. B., Garrison, E. P., Crawford, D. A., Kelly, B. D., Shindle, D. B.,

534   Godsea, K. G., Miller, K. V., & Conner, L. M. (2018). Wildfire affects space use and

535   movement of white-tailed deer in a tropical pyric landscape. Forest Ecology and

536   Management, 409, 161–169. https://doi.org/10.1016/j.foreco.2017.11.007

537   de Valpine, P., Turek, D., Paciorek, C. J., Anderson-Bergman, C., Lang, D. T., & Bodik, R.

538   (2017). Programming With Models: Writing Statistical Algorithms for General Model

539   Structures With NIMBLE. Journal of Computational and Graphical Statistics, 26(2),

540   403–413. https://doi.org/10.1080/10618600.2016.1172487

541   Devarajan, K., Morelli, T. L., & Tenan, S. (2020). Multi-species occupancy models: Review,

542   roadmap, and recommendations. Ecography, 43(11), 1612–1624.

543   https://doi.org/10.1111/ecog.04957

544   Doherty, T. S., Geary W. L., Jolly, C. J., Macdonald, K. J., Miritis, V., Watchorn, D. J., Cherry,

545   M. J., Conner, L. M., González, T. M., Legge, S. M., Ritchie, E. G., Stawski, C., and

546   Dickman, C.R. (2022). Fire as a driver and mediator of predator-prey interactions.

547   Biological Reviews. https://doi.org/10.1111/brv.12853.

548   Eastburn, D. J., O'Geen, A. T., Tate, K. W., & Roche, L. M. (2017). Multiple ecosystem services

549   in a working landscape. PLOS ONE, 12(3), e0166595.

550   https://doi.org/10.1371/journal.pone.0166595

551   ESRI 2011. ArcGIS Desktop: Release 10. Redlands, CA: Environmental Systems Research

552   Institute.

553   Estes, J. A., Terborgh, J., Brashares, J. S., Power, M. E., Berger, J., Bond, W. J., Carpenter, S.

554   R., Essington, T. E., Holt, R. D., Jackson, J. B. C., Marquis, R. J., Oksanen, L., Oksanen,

555   T., Paine, R. T., Pikitch, E. K., Ripple, W. J., Sandin, S. A., Scheffer, M., Schoener, T.

556   W., … Wardle, D. A. (2011). Trophic Downgrading of Planet Earth. Science, 333(6040),

557   301–306. https://doi.org/10.1126/science.1205106

558   Furnas, B. J., Goldstein, B. R., & Figura, P. J. (2021). Intermediate fire severity diversity

559   promotes richness of forest carnivores in California. Diversity and Distributions,

560   ddi.13374. https://doi.org/10.1111/ddi.13374

561   Gaynor, K. M., Daskin, J. H., Rich, L. N., & Brashares, J. S. (2021). Postwar wildlife recovery in

562   an African savanna: Evaluating patterns and drivers of species occupancy and richness.

563   Animal Conservation, 24(3), 510–522. https://doi.org/10.1111/acv.12661

564   Geary, W. L., Doherty, T. S., Nimmo, D. G., Tulloch, A. I. T., & Ritchie, E. G. (2020). Predator

565   responses to fire: A global systematic review and meta-analysis. Journal of Animal

566   Ecology, 89(4), 955–971. https://doi.org/10.1111/1365-2656.13153

567   Gelman, A., Carlin, J.B., Stern, H.S. & Rubin, D.B. (2004). Bayesian data analysis. Boca Raton,

568   FL: Chapman and Hall.

569   Gelman, A., Hwang, J., & Vehtari, A. (2014). Understanding predictive information criteria for

570   Bayesian models. Statistics and Computing, 24(6), 997–1016.

571   https://doi.org/10.1007/s11222-013-9416-2

572   Gelman, A., Meng, X.-L., & Stern, H. (1996). Posterior predictive assessment of model fitness

573   via realized discrepancies. 76.

574 Gigliotti, L. C., Curveira-Santos, G., Slotow, R., Sholto-Douglas, C., Swanepoel, L. H., &

575   Jachowski, D. S. (2022). Community-level responses of African carnivores to prescribed

576   burning. *Journal of Applied Ecology*, *59*(1), 251-262.

577 Goldstein B, Turek D, Ponisio L, de Valpine P (2021). "nimbleEcology: Distributions for

578   Ecological Models in nimble." R package version 0.4.1, <https://cran.r-

579   project.org/package=nimbleEcology>.

580 González, T. M., González-Trujillo, J. D., Muñoz, A., & Armenteras, D. (2022). Effects of fire

581   history on animal communities: A systematic review. Ecological Processes, 11(1), 11.

582   https://doi.org/10.1186/s13717-021-00357-7

583 Heller, N. E., & Zavaleta, E. S. (2009). Biodiversity management in the face of climate change:

584   A review of 22 years of recommendations. Biological Conservation, 142(1), 14–32.

585   https://doi.org/10.1016/j.biocon.2008.10.006

586 Hill, J. E., DeVault, T. L., & Belant, J. L. (2021). A review of ecological factors promoting road

587   use by mammals. Mammal Review, 51(2), 214–227. https://doi.org/10.1111/mam.12222

588 Holling, C. S. (1973). Resilience and Stability of Ecological Systems. 24.

589 Iknayan, K. J., Tingley, M. W., Furnas, B. J., & Beissinger, S. R. (2014). Detecting diversity:

590   Emerging methods to estimate species diversity. Trends in Ecology & Evolution, 29(2),

591   97–106. https://doi.org/10.1016/j.tree.2013.10.012

592 Ingrisch, J., & Bahn, M. (2018). Towards a Comparable Quantification of Resilience. Trends in

593   Ecology & Evolution, 33(4), 251–259. https://doi.org/10.1016/j.tree.2018.01.013

594 Jager, H. I., Long, J. W., Malison, R. L., Murphy, B. P., Rust, A., Silva, L. G. M., Sollmann, R.,

595   Steel, Z. L., Bowen, M. D., Dunham, J. B., Ebersole, J. L., & Flitcroft, R. L. (2021).

596   Resilience of terrestrial and aquatic fauna to historical and future wildfire regimes in

597   western North America. Ecology and Evolution, 11(18), 12259–12284.

598   https://doi.org/10.1002/ece3.8026

599   Jennings, M. K., Lewison, R. L., Vickers, T. W., & Boyce, W. M. (2016). Puma response to the

600   effects of fire and urbanization. The Journal of Wildlife Management, 80(2), 221–234.

601   https://doi.org/10.1002/jwmg.1018

602   Jolly, C. J., Dickman, C. R., Doherty, T. S., Eeden, L. M., Geary, W. L., Legge, S. M.,

603   Woinarski, J. C. Z., & Nimmo, D. G. (2022). Animal mortality during fire. Global

604   Change Biology, gcb.16044. https://doi.org/10.1111/gcb.16044

605   Kays, R., Arbogast, B. S., Baker-Whatton, M., Beirne, C., Boone, H. M., Bowler, M., Burneo, S.

606   F., Cove, M. V., Ding, P., Espinosa, S., Gonçalves, A. L. S., Hansen, C. P., Jansen, P. A.,

607   Kolowski, J. M., Knowles, T. W., Lima, M. G. M., Millspaugh, J., McShea, W. J.,

608   Pacifici, K., … Spironello, W. R. (2020). An empirical evaluation of camera trap study

609   design: How many, how long and when? Methods in Ecology and Evolution, 11(6), 700–

610   713. https://doi.org/10.1111/2041-210X.13370

611   Keeley, J. (2009). Fire intensity, fire severity and burn severity: a brief review and suggested

612   usage. *International journal of wildland fire*, *18*(1), 116-126.

613   Kelly, L. T., Giljohann, K. M., Duane, A., Aquilué, N., Archibald, S., Batllori, E., Bennett, A. F.,

614   Buckland, S. T., Canelles, Q., Clarke, M. F., Fortin, M.-J., Hermoso, V., Herrando, S.,

615   Keane, R. E., Lake, F. K., McCarthy, M. A., Morán-Ordóñez, A., Parr, C. L., Pausas, J.

616   G., … Brotons, L. (2020). Fire and biodiversity in the Anthropocene. Science, 370(6519),

617   eabb0355. https://doi.org/10.1126/science.abb0355

618   Kreling, S. E. S., Gaynor, K. M., McInturff, A., Calhoun, K. L., & Brashares, J. S. (2021). Site

619   fidelity and behavioral plasticity regulate an ungulate's response to extreme disturbance.

620   Ecology and Evolution, 11(22), 15683–15694. https://doi.org/10.1002/ece3.8221

621   Li, S., & Banerjee, T. (2021). Spatial and temporal pattern of wildfires in California from 2000

622   to 2019. Scientific Reports, 11(1), 8779. https://doi.org/10.1038/s41598-021-88131-9

623   MacKenzie, D. I., Nichols, J. D., Lachman, G. B., Droege, S., Andrew Royle, J., & Langtimm,

624   C. A. (2002). Estimating Site Occupancy Rates When Detection Probabilities Are Less

625   Than One. Ecology, 83(8), 2248–2255. https://doi.org/10.1890/0012-

626   9658(2002)083[2248:ESORWD]2.0.CO;2

627   MacKenzie, D. I., Nichols, J. D., Royle, J. A., Pollock, K. H., Bailey, L. L., & Hines, J. E.

628   (2017). *Occupancy estimation and modeling: inferring patterns and dynamics of species*

629   *occurrence*. Elsevier.

630   McWethy, D. B., Schoennagel, T., Higuera, P. E., Krawchuk, M., Harvey, B. J., Metcalf, E. C.,

631   Schultz, C., Miller, C., Metcalf, A. L., Buma, B., Virapongse, A., Kulig, J. C., Stedman,

632   R. C., Ratajczak, Z., Nelson, C. R., & Kolden, C. (2019). Rethinking resilience to

633   wildfire. Nature Sustainability, 2(9), 797–804. https://doi.org/10.1038/s41893-019-0353-

634   8

635   Miller, C., Higuera, P. E., McWethy, D. B., Metcalf, A. L., Metcalf, E. C., Black, A. E., Clarke,

636   L., & Hodge, H. (2021). Developing strategies to support social-ecological resilience in

637   flammable landscapes: A structured approach for natural resource managers and other

638   stakeholders (RMRS-RN-92; p. RMRS-RN-92). U.S. Department of Agriculture, Forest

639   Service, Rocky Mountain Research Station. https://doi.org/10.2737/RMRS-RN-92

640   Neilson, E. W., Avgar, T., Burton, A. C., Broadley, K., & Boutin, S. (2018). Animal movement

641   affects interpretation of occupancy models from camera-trap surveys of unmarked

642   animals. Ecosphere, 9(1). https://doi.org/10.1002/ecs2.2092

643   Niedballa, J., Sollmann, R., Courtiol, A., & Wilting, A. (2016). camtrapR: An R package for

644   efficient camera trap data management. Methods in Ecology and Evolution, 7(12), 1457–

645   1462. https://doi.org/10.1111/2041-210X.12600

646   Nimmo, D. G., Avitabile, S., Banks, S. C., Bliege Bird, R., Callister, K., Clarke, M. F., Dickman,

647   C. R., Doherty, T. S., Driscoll, D. A., Greenville, A. C., Haslem, A., Kelly, L. T., Kenny,

648   S. A., Lahoz-Monfort, J. J., Lee, C., Leonard, S., Moore, H., Newsome, T. M., Parr, C.

649   L., … Bennett, A. F. (2019). Animal movements in fire-prone landscapes. Biological

650   Reviews, 94(3), 981–998. https://doi.org/10.1111/brv.12486

651   Nimmo, D. G., Carthey, A. J., Jolly, C. J., & Blumstein, D. T. (2021). Welcome to the

652   Pyrocene: Animal survival in the age of megafire. *Global Change Biology*, *27*(22), 5684-

653   5693.

654   Northrup, J. M., & Gerber, B. D. (2018). A comment on priors for Bayesian occupancy models.

655   PLOS ONE, 13(2), e0192819. https://doi.org/10.1371/journal.pone.0192819

656   Pimm, S. L. (1984). The complexity and stability of ecosystems. *Nature*, *307*(5949), 321-326.

657   Planet Team (2017). Planet Application Program Interface: In Space for Life on Earth. San

658   Francisco, CA. https://api.planet.com.

659   Poley, L. G., Pond, B. A., Schaefer, J. A., Brown, G. S., Ray, J. C., & Johnson, D. S. (2014).

660   Occupancy patterns of large mammals in the Far North of Ontario under imperfect

661   detection and spatial autocorrelation. *Journal of Biogeography*, *41*(1), 122-132.

662   Reiss, M. (1988). Scaling of home range size: body size, metabolic needs and ecology. *Trends in*

663   *Ecology & Evolution*, *3*(3), 85-86.

664   Rich, L. N., Beissinger, S. R., Brashares, J. S., & Furnas, B. J. (2019). Artificial water

665   catchments influence wildlife distribution in the Mojave Desert. The Journal of Wildlife

666   Management, 83(4), 855–865. https://doi.org/10.1002/jwmg.21654

667   Royle, J. A. (2004). N -Mixture Models for Estimating Population Size from Spatially

668   Replicated Counts. Biometrics, 60(1), 108–115. https://doi.org/10.1111/j.0006-

669   341X.2004.00142.x

670   Royle, J. A., & Nichols, J. D. (2003). Estimating abundance from repeated presence-abcence

671   data or point counts. Ecology, 84(3), 777–790. https://doi.org/10.1890/0012-

672   9658(2003)084[0777:EAFRPA]2.0.CO;2

673   Schuette, P. A., Diffendorfer, J. E., Deutschman, D. H., Tremor, S., & Spencer, W. (2014).

674   Carnivore distributions across chaparral habitats exposed to wildfire and rural housing in

675   southern California. International Journal of Wildland Fire, 23(4), 591.

676   https://doi.org/10.1071/WF13062

677   Sentinel Hub (2021). Modified Copernicus Sentinel Data. https://www.sentinel-hub.com

678   Soga, M., & Gaston, K. J. (2018). Shifting baseline syndrome: Causes, consequences, and

679   implications. Frontiers in Ecology and the Environment, 16(4), 222–230.

680   https://doi.org/10.1002/fee.1794

681   Standish, R. J., Hobbs, R. J., Mayfield, M. M., Bestelmeyer, B. T., Suding, K. N., Battaglia, L.

682   L., Eviner, V., Hawkes, C. V., Temperton, V. M., Cramer, V. A., Harris, J. A., Funk, J.

683   L., & Thomas, P. A. (2014). Resilience in ecology: Abstraction, distraction, or where the

684   action is? Biological Conservation, 177, 43–51.

685   https://doi.org/10.1016/j.biocon.2014.06.008

686   Steel, Z. L., Fogg, A. M., Burnett, R., Roberts, L. J., & Safford, H. D. (2021). When bigger isn't

687   better—Implications of large high-severity wildfire patches for avian diversity and

688   community composition. Diversity and Distributions, ddi.13281.

689   https://doi.org/10.1111/ddi.13281

690   Stephens, S. L., Burrows, N., Buyantuyev, A., Gray, R. W., Keane, R. E., Kubian, R., Liu, S.,

691   Seijo, F., Shu, L., Tolhurst, K. G., & van Wagtendonk, J. W. (2014). Temperate and

692   boreal forest mega-fires: Characteristics and challenges. Frontiers in Ecology and the

693   Environment, 12(2), 115–122. https://doi.org/10.1890/120332

694   Sunde, M. G., Diamond, D. D., Elliott, L. F., Hanberry, P., & True, D. (2020). Mapping high-

695   resolution percentage canopy cover using a multi-sensor approach. Remote Sensing of

696   Environment, 242, 111748. https://doi.org/10.1016/j.rse.2020.111748

697   Suraci, J. P., Gaynor, K. M., Allen, M. L., Alexander, P., Brashares, J. S., Cendejas-Zarelli, S.,

698   Crooks, K., Elbroch, L. M., Forrester, T., Green, A. M., Haight, J., Harris, N. C.,

699   Hebblewhite, M., Isbell, F., Johnston, B., Kays, R., Lendrum, P. E., Lewis, J. S.,

700   McInturff, A., … Wilmers, C. C. (2021). Disturbance type and species life history predict

701   mammal responses to humans. Global Change Biology, 27(16), 3718–3731.

702   https://doi.org/10.1111/gcb.15650

703   Syphard, A. D., & Keeley, J. E. (2020). Mapping fire regime ecoregions in

704   California. *International Journal of Wildland Fire*, *29*(7), 595-601.

705   Tilahun, A., & Teferie, B. (2015). Accuracy assessment of land use land cover classification

706   using Google Earth. *American Journal of Environmental Protection*, *4*(4), 193-198.

707   Veldman, J. W., Buisson, E., Durigan, G., Fernandes, G. W., Le Stradic, S., Mahy, G., ... &

708   Bond, W. J. (2015). Toward an old-growth concept for grasslands, savannas, and

709   woodlands. *Frontiers in Ecology and the Environment*, *13*(3), 154-162.

710

711

712

713

714

715

716

717

718

719

720

721

722

723

724

725

726

727

728

729

730

731 Tables

Species	Resistant?	Resilient?	Species	Resistant?	Resilient?
Bear	✗	✓	Ground Squirrel	✓	✓
Bobcat	✓	✓	Jackrabbit	✓	✓
Coyote	✓	✓	Mountain Lion	✗	✓
Deer	✗	✓	Wild Boar	✓	✓
Fox	✓	✓	Raccoon	✗	✗
Gray Squirrel	✗	✗	Skunk	✓	✓

732

733 Table 1 – Summarized assessment of species-specific resistance and resilience to megafire. For

734 the purposes of our study, we deemed species "resilient" if the species' single species occupancy

735 model estimated no effect of burn history on intensity of use or occupancy in the years since

736 burn, or if we observed an increase in these estimates relative to unburned sites. We deemed

737 species "resistant" to fire if the species' single species occupancy model estimated no effect of

738 burn history on intensity of use or occupancy, or if either of these estimates increased relative to

739 unburned sites during the year of the fire.

740

741

742

743

744

745

746

747

748

749

750

751

752

753

754

755

756

757

758

759   Figure Captions

760   Figure 1 – Maps of the 2018 Mendocino Complex Fire and the study site, the U.C. Hopland

761   Research and Extension Center (HREC) (39°00′ N, 123°04' W). Map "a" displays the total burn

762   perimeter of the Mendocino Complex Fire, composed of the northern Ranch fire and the

763   southern River Fire. The River Fire burned half of the center property. Map "b" displays the

764   change in canopy cover caused by the 2018 River Fire in addition to the Center's camera grid.

765   Change in canopy cover was associated with burn severity – a burn severity map of the region

766   can be found in Appendix 1 - Figure S1.1.

767

768   Figure 2 – Detection Rate (number of detections/sampling nights) for each examined species

769   across each year's sampling period (Oct 1st – Nov 31st) for all cameras. Dashed line at "2018"

770   represents the year of the Mendocino Complex Fire (July 27th, 2018). Note that the y-axis scale

771   differs between species in order to improve visualization of relative change in detection rate

772   within each species.

773

774   Figure 3 – Predicted probability of detection (intensity of use) with 90% credible intervals at

775   each camera site under each burn history category across all study species. All other detection

776   covariates were set to their mean values.

777

778   Figure 4 - Community richness estimates from the multi-species occupancy model (MSOM)

779   across "time since burned" categories and canopy cover. All other detection covariates were set

780   to their mean values. Panel "a" corresponds to all sites that were unburned by the fire. Panel "b"

781   corresponds to sites that were burned during the year of the fire (2018). Panels "c" and "d"

782   correspond to sites that were burned 1-year (2019) and 2-years (2020) post-fire respectively.

783

784

785

786

787

788

789
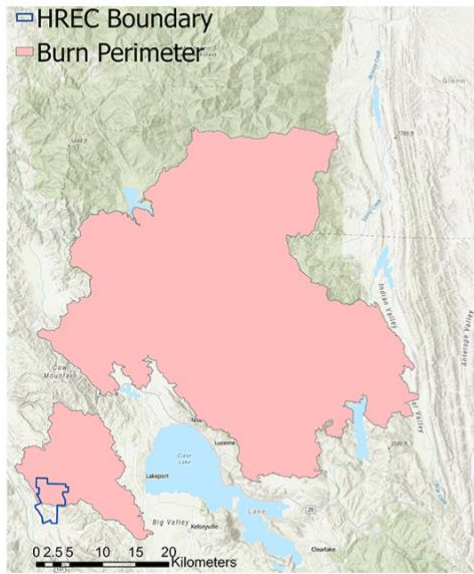
790

791

792

793

794

795
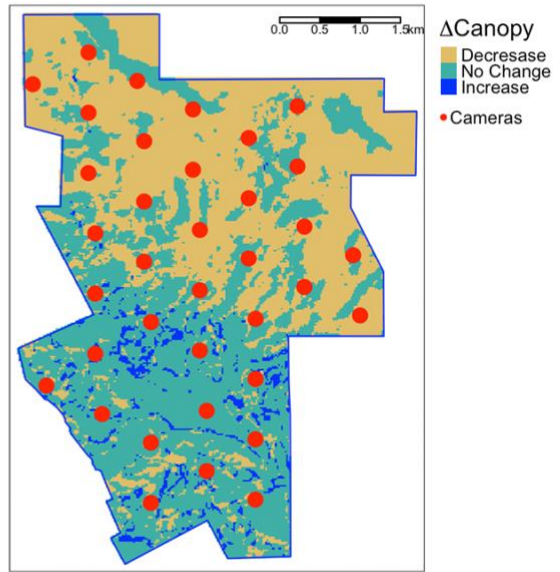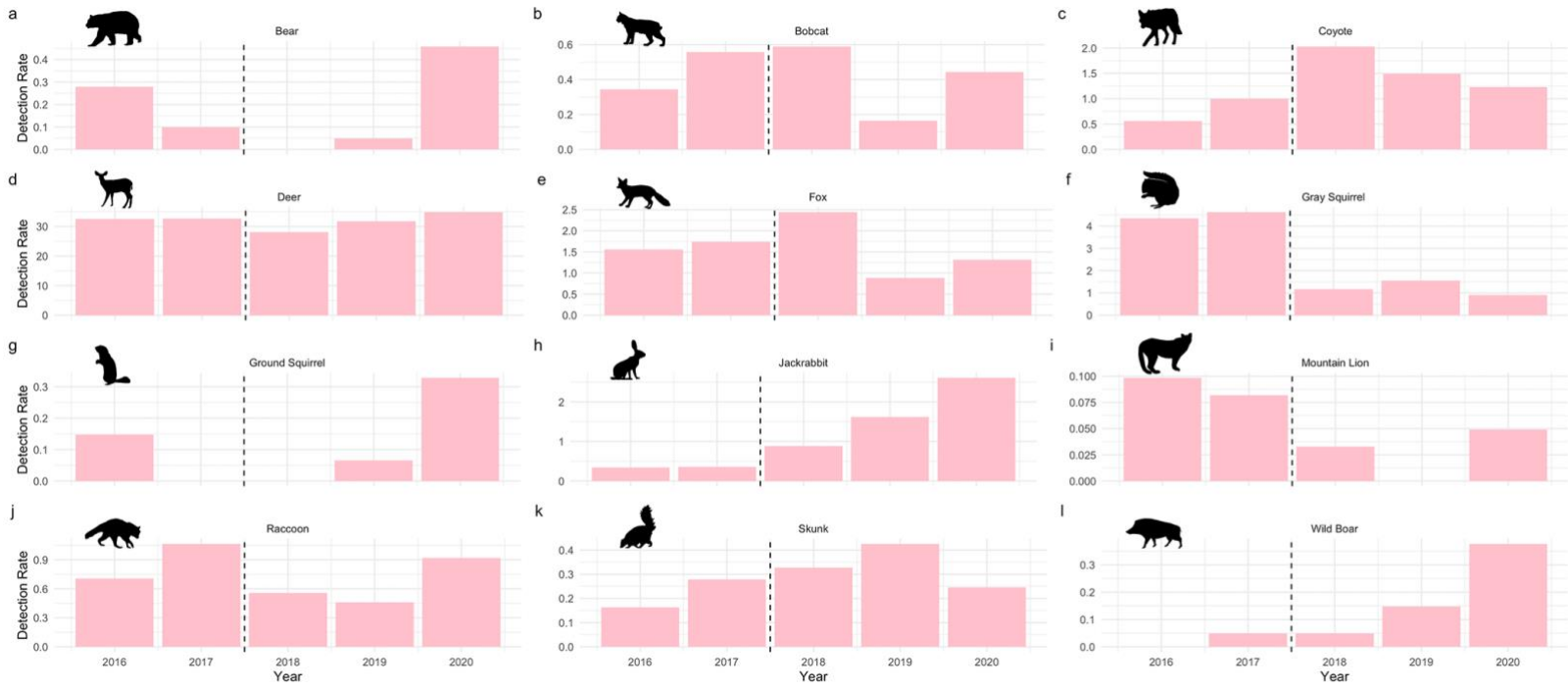
796

797

798

799

800

801

802

803

804   Figure 1

813 Figure 2
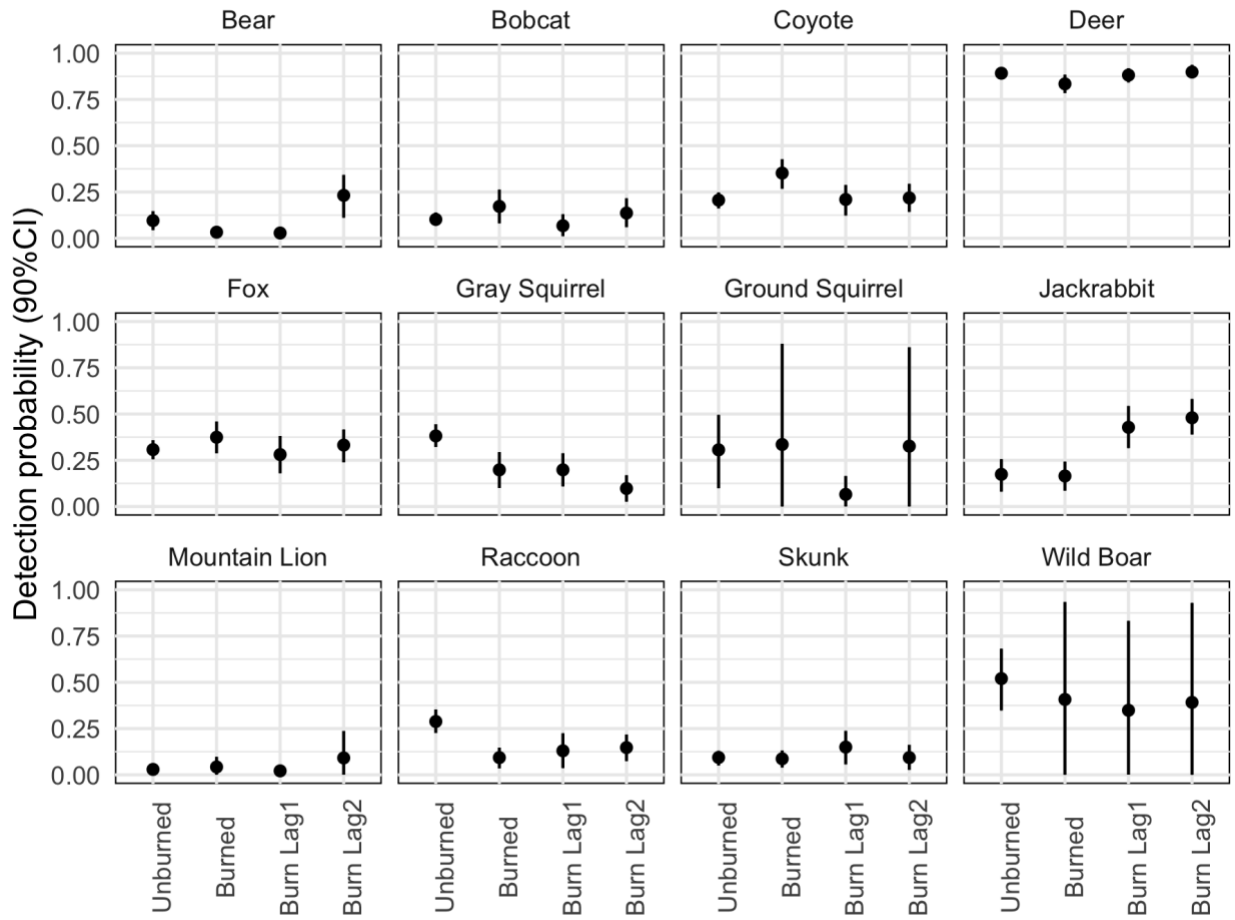
Figure 3

836   Figure 4
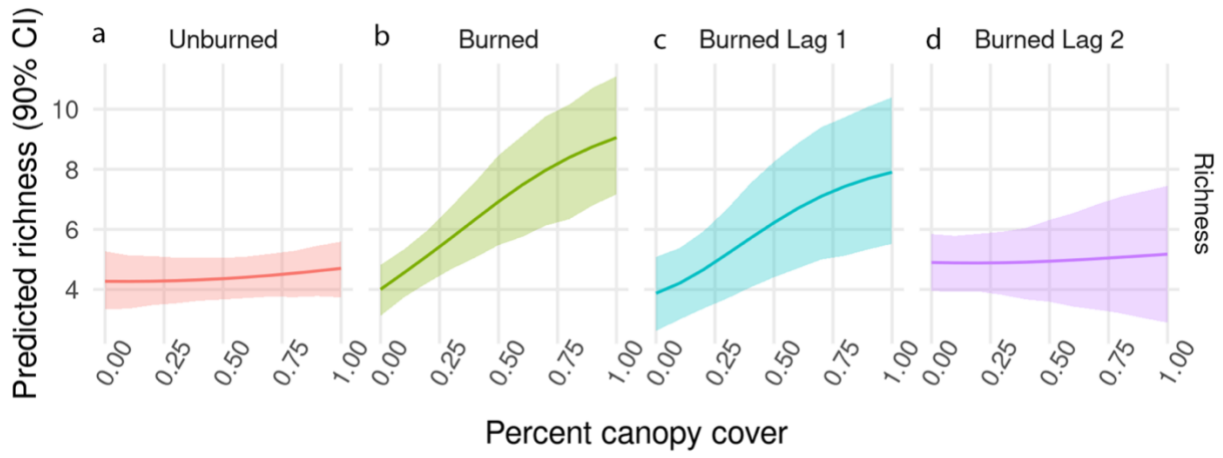
853   Authors: Kendall L. Calhoun, Benjamin R. Goldstein, Kaitlyn M. Gaynor, Alex McInturff,

854   Leonel Solorio, Justin S. Brashares

855   Title: Mammalian resilience to megafire in western U.S. woodland savannas

857

858   **Supplement 1 – Additional Figures and Tables**

859
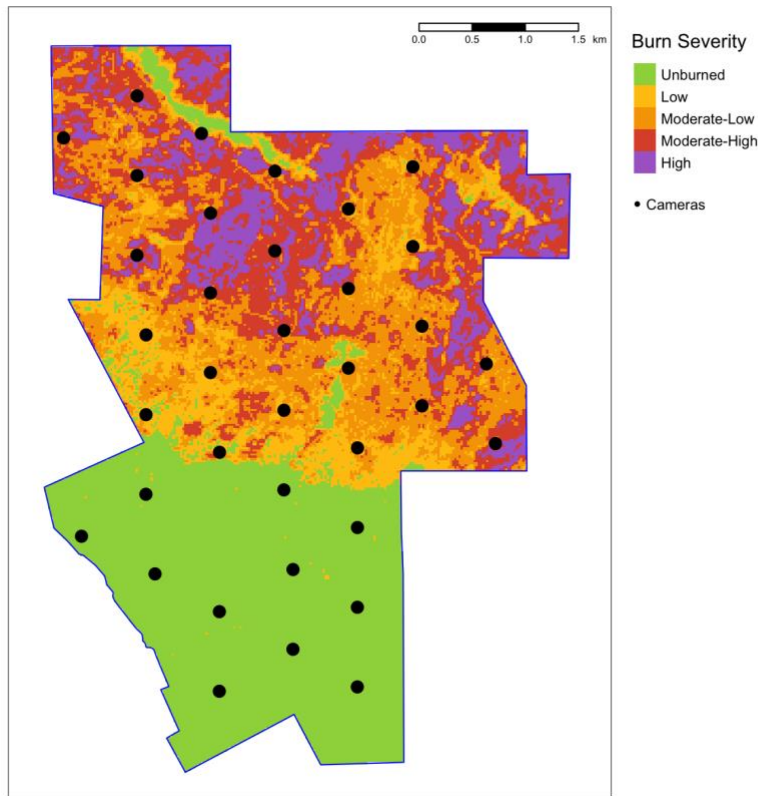
860
861

862   Figure S1.1 –Burn severity (ΔNormalized Burn Ratio) map of the River Fire within the Hopland

863   Research and Extension Center (HREC) (39°00′ N, 123°04' W). The Normalized Burn Ratio

864   (NBR) was created using Sentinel-2 imagery (Sentinel Hub, 2021) (10m resolution) collected

865   both before and after the fire. Delta NBR was calculated using the following equations (Keeley,

866   2009):

867      $$\Delta NBR = NBR_{prefire} - NBR_{postfire}$$

868      $NBR = Near\text{-}infrared\ (NIR) - shortwave\ infrared\ (SWIR)\ /\ Near\text{-}infrared\ (NIR) + shortwave$

869      $infrared\ (SWIR)$

870
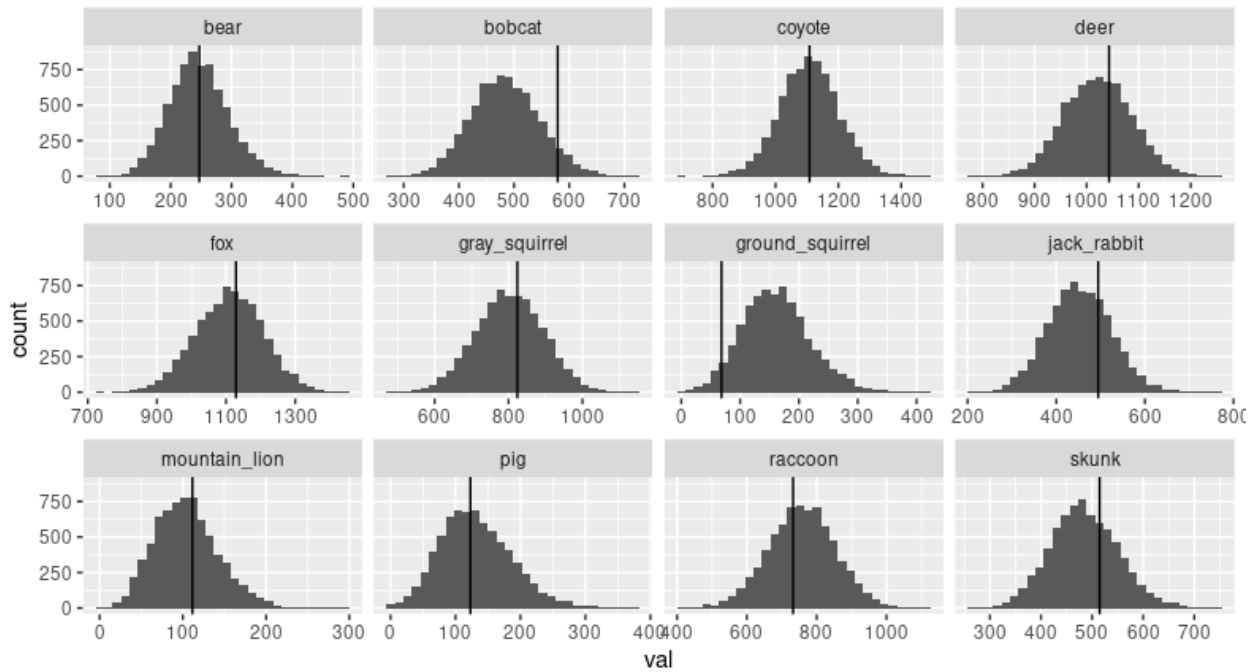
871
872
873   Figure S1.2 - Observed deviances of fit models did not visibly differ from the posterior

874   distributions of deviances generated from simulated datasets, meaning that we found no evidence

875   of poor model fit.

876

Species	Total # Detected	Species	Total # Detected
Black Bear	**55**	**Ground Squirrel**	**34**
Bobcat	**130**	**Jackrabbit**	**364**
Coyote	**387**	**Mountain Lion**	**16**
BT Deer	**7908**	**Wild Pig**	**39**
Gray Fox	**496**	**Raccoon**	**231**
Gray Squirrel	**787**	**Skunk**	**88**

877
878   Table S1.1 - Total number of independent detections by camera traps for each of the 12 studied

879   species. Species detections were considered independent if species were detected at least 15

880   minutes after the previous detection of the same species at the same site.

881
882
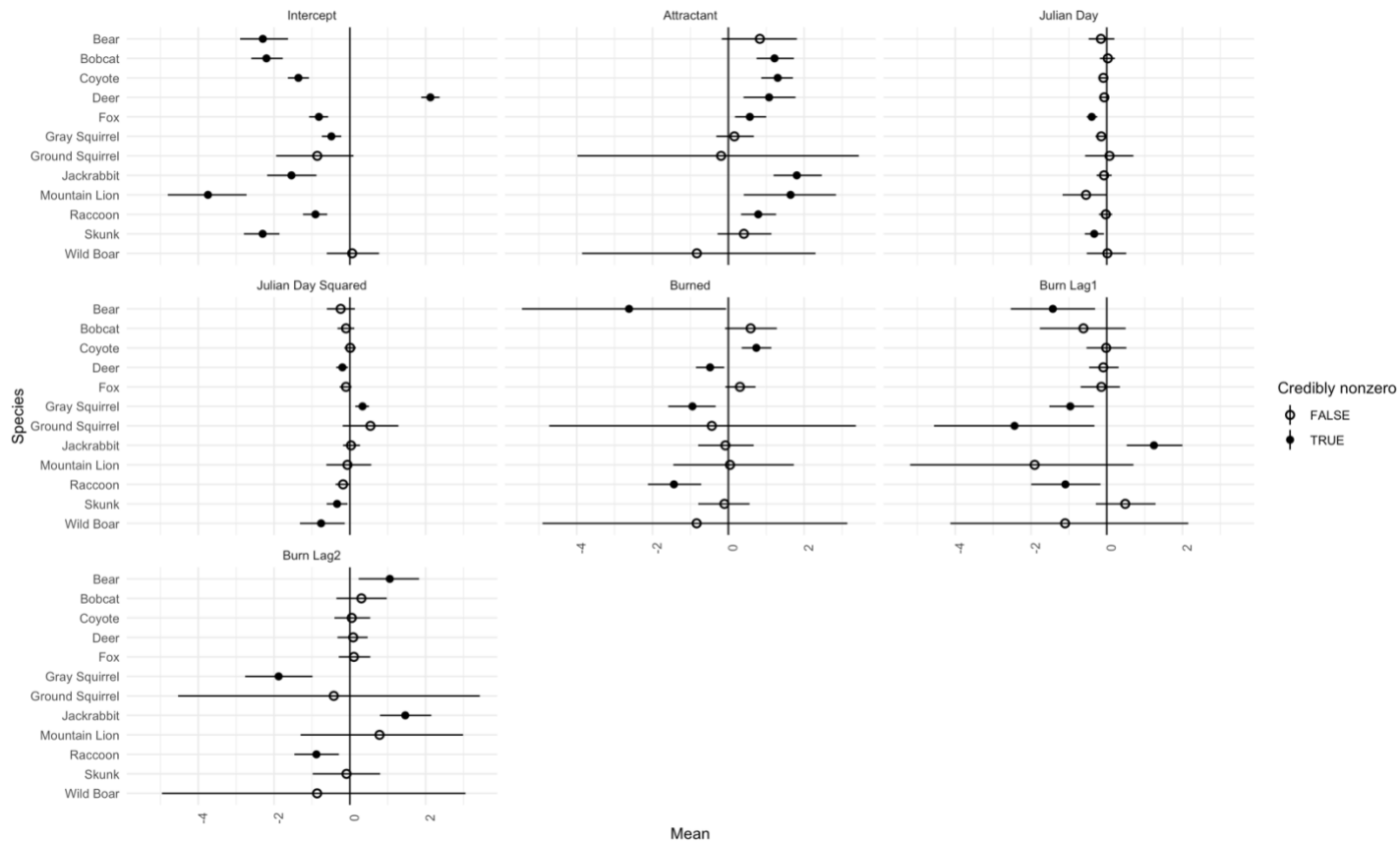
883
884
885   Figure S1.3 – Plotted coefficients of all detection covariates for single species occupancy model

886   (SSOM) across each species.

887

Species	Parameter	Estimate	Species	Parameter	Estimate
Bear	Intercept	-2.31 (-2.93, -1.66)	Ground Squirrel	Intercept	-0.89 (-1.93, 0.12)
Bear	Attractant	0.81 (-0.21, 1.8)	Ground Squirrel	Attractant	-0.18 (-4.2, 3.24)
Bear	Julian Day	-0.16 (-0.49, 0.19)	Ground Squirrel	Julian Day	0.07 (-0.53, 0.7)
Bear	Julian Day Sq	-0.24 (-0.6, 0.13)	Ground Squirrel	Julian Day Sq	0.56 (-0.19, 1.28)
Bear	Burned	-2.54 (-5.45, -0.04)	Ground Squirrel	Burned	-0.47 (-4.64, 3.5)
Bear	Burn Lag1	-1.44 (-2.58, -0.34)	Ground Squirrel	Burn Lag1	-2.42 (-4.56, -0.42)
Bear	Burn Lag2	1.07 (0.25, 1.84)	Ground Squirrel	Burn Lag2	-0.54 (-4.52, 3.58)

Bobcat	Intercept	-2.2 (-2.63, -1.82)	Jackrabbit	Intercept	-1.61 (-2.26, -0.95)
Bobcat	Attractant	1.23 (0.73, 1.72)	Jackrabbit	Attractant	1.83 (1.17, 2.42)
Bobcat	Julian Day	0.03 (-0.17, 0.24)	Jackrabbit	Julian Day	-0.07 (-0.26, 0.14)
Bobcat	Julian Day Sq	-0.1 (-0.31, 0.14)	Jackrabbit	Julian Day Sq	0.04 (-0.19, 0.25)
Bobcat	Burned	0.58 (-0.07, 1.24)	Jackrabbit	Burned	-0.06 (-0.84, 0.65)
Bobcat	Burn Lag1	-0.62 (-1.7, 0.55)	Jackrabbit	Burn Lag1	1.31 (0.59, 2.04)
Bobcat	Burn Lag2	0.29 (-0.37, 0.96)	Jackrabbit	Burn Lag2	1.53 (0.84, 2.21)
Coyote	Intercept	-1.36 (-1.63, -1.09)	Mountain Lion	Intercept	-3.69 (-4.75, -2.64)
Coyote	Attractant	1.3 (0.89, 1.72)	Mountain Lion	Attractant	1.63 (0.43, 2.86)
Coyote	Julian Day	-0.09 (-0.22, 0.04)	Mountain Lion	Julian Day	-0.55 (-1.13, 0.05)
Coyote	Julian Day Sq	0.01 (-0.14, 0.16)	Mountain Lion	Julian Day Sq	-0.08 (-0.69, 0.54)
Coyote	Burned	0.74 (0.37, 1.14)	Mountain Lion	Burned	0.02 (-1.62, 1.7)
Coyote	Burn Lag1	0 (-0.53, 0.52)	Mountain Lion	Burn Lag1	-1.89 (-5.14, 0.7)
Coyote	Burn Lag2	0.06 (-0.4, 0.54)	Mountain Lion	Burn Lag2	0.72 (-1.21, 3.13)
Deer	Intercept	2.12 (1.87, 2.34)	Wild Boar	Intercept	0.08 (-0.63, 0.76)
Deer	Attractant	1.08 (0.34, 1.76)	Wild Boar	Attractant	-0.84 (-3.91, 2.21)
Deer	Julian Day	-0.06 (-0.2, 0.07)	Wild Boar	Julian Day	0 (-0.56, 0.51)
Deer	Julian Day Sq	-0.19 (-0.35, -0.05)	Wild Boar	Julian Day Sq	-0.78 (-1.35, -0.14)
Deer	Burned	-0.48 (-0.85, -0.1)	Wild Boar	Burned	-0.82 (-4.85, 3.33)
Deer	Burn Lag1	-0.09 (-0.47, 0.29)	Wild Boar	Burn Lag1	-1.11 (-4.21, 2.06)
Deer	Burn Lag2	0.09 (-0.34, 0.49)	Wild Boar	Burn Lag2	-0.92 (-5.03, 3.12)

Fox	Intercept	-0.82 (-1.07, -0.58)	Raccoon	Intercept	-0.91 (-1.22, -0.6)
Fox	Attractant	0.57 (0.17, 1.01)	Raccoon	Attractant	0.81 (0.33, 1.24)
Fox	Julian Day	-0.4 (-0.54, -0.26)	Raccoon	Julian Day	-0.02 (-0.19, 0.16)
Fox	Julian Day Sq	-0.1 (-0.27, 0.05)	Raccoon	Julian Day Sq	-0.18 (-0.38, 0.02)
Fox	Burned	0.3 (-0.07, 0.71)	Raccoon	Burned	-1.44 (-2.11, -0.68)
Fox	Burn Lag1	-0.15 (-0.68, 0.38)	Raccoon	Burn Lag1	-1.11 (-2.04, -0.25)
Fox	Burn Lag2	0.11 (-0.31, 0.52)	Raccoon	Burn Lag2	-0.89 (-1.48, -0.31)
Gray Squirrel	Intercept	-0.49 (-0.74, -0.22)	Skunk	Intercept	-2.3 (-2.77, -1.8)
Gray Squirrel	Attractant	0.16 (-0.33, 0.63)	Skunk	Attractant	0.42 (-0.29, 1.13)
Gray Squirrel	Julian Day	-0.14 (-0.3, 0)	Skunk	Julian Day	-0.33 (-0.58, -0.07)
Gray Squirrel	Julian Day Sq	0.34 (0.14, 0.52)	Skunk	Julian Day Sq	-0.34 (-0.62, -0.07)
Gray Squirrel	Burned	-0.96 (-1.58, -0.33)	Skunk	Burned	-0.11 (-0.78, 0.6)
Gray Squirrel	Burn Lag1	-0.95 (-1.56, -0.41)	Skunk	Burn Lag1	0.49 (-0.3, 1.28)
Gray Squirrel	Burn Lag2	-1.86 (-2.73, -0.94)	Skunk	Burn Lag2	-0.09 (-1, 0.82)

888
889   Table S1.2 – Coefficients for detection covariates for each Single-species Occupancy Model.

890   Coefficient estimates, as well as upper and lower credible intervals are listed for each covariate

891   and for each species.

892
893
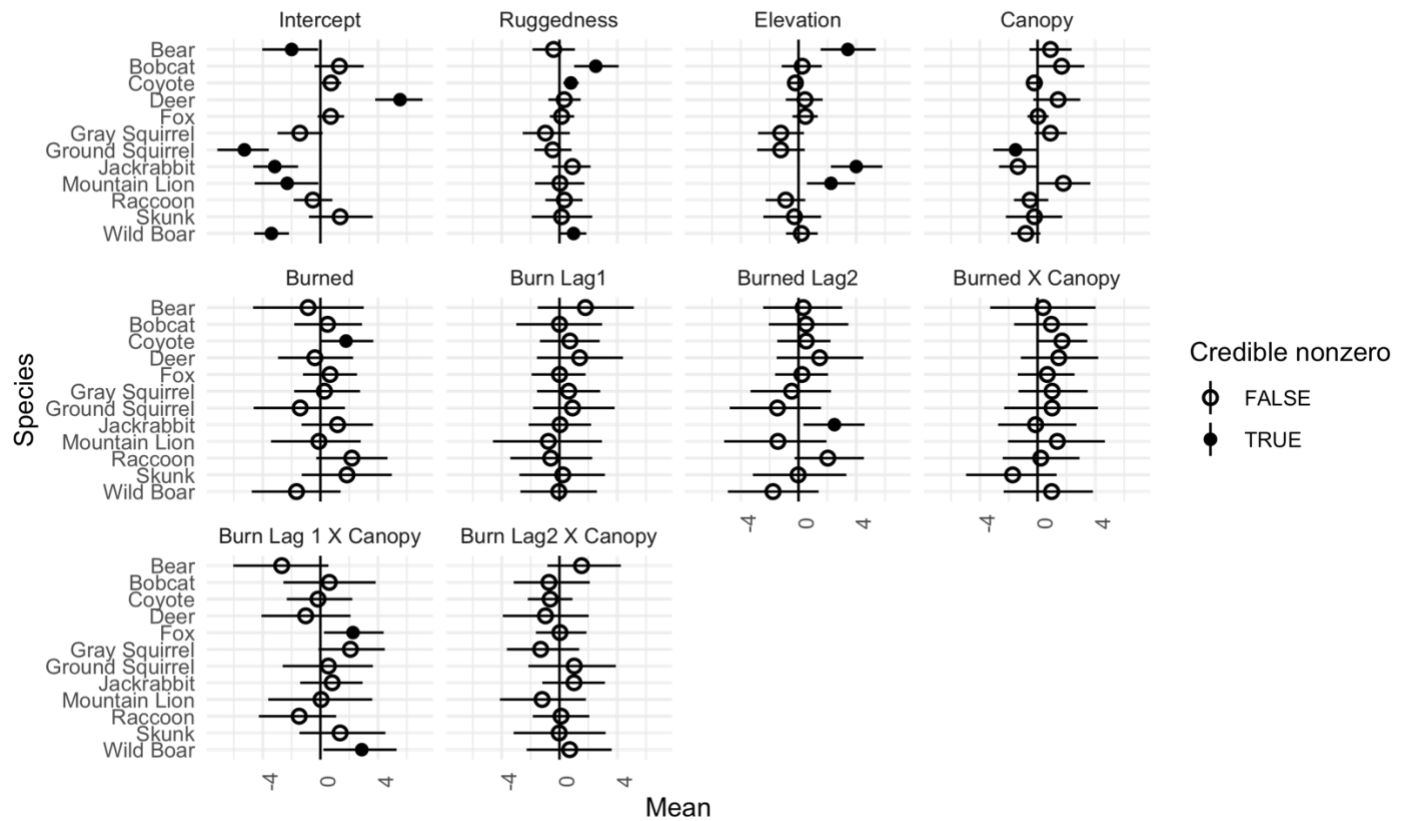
894
895
896   Figure S1.4 – Plotted coefficients of all occupancy covariates for each single species occupancy

897   model (SSOM) for each species.

898

Species	Parameter	Estimate	Species	Parameter	Estimate
Bear	Intercept	-1.99 (-4.03, -0.15)	Ground Squirrel	Intercept	-5.27 (-7.15, -3.58)
Bear	Ruggedness	-0.41 (-1.87, 1.08)	Ground Squirrel	Ruggedness	-0.47 (-1.75, 0.84)
Bear	Elevation	3.42 (1.53, 5.35)	Ground Squirrel	Elevation	-1.23 (-2.87, 0.44)
Bear	Canopy	0.9 (-0.57, 2.36)	Ground Squirrel	Canopy	-1.52 (-3.07, -0.02)
Bear	Burned	-0.85 (-4.67, 3)	Ground Squirrel	Burned	-1.4 (-4.63, 1.71)
Bear	Burn Lag1	1.8 (-1.51, 5.16)	Ground Squirrel	Burn Lag1	0.9 (-1.83, 3.82)
Bear	Burn Lag2	0.32 (-2.46, 3.04)	Ground Squirrel	Burn Lag2	-1.46 (-4.77, 1.56)
Bear	Burned X Canopy	0.38 (-3.29, 4.03)	Ground Squirrel	Burned X Canopy	1.01 (-2.32, 4.19)
Bear	Burn Lag1 X Canopy	-2.68 (-6.04, 0.56)	Ground Squirrel	Burn Lag1 X Canopy	0.55 (-2.62, 3.64)

Bear	Burn Lag2 X Canopy	1.53 (-0.83, 4.26)	Ground Squirrel	Burn Lag2 X Canopy	1.02 (-2.15, 3.91)
Bobcat	Intercept	1.32 (-0.41, 3)	Jackrabbit	Intercept	-3.16 (-4.66, -1.54)
Bobcat	Ruggedness	2.52 (1.01, 4.11)	Jackrabbit	Ruggedness	0.9 (-0.52, 2.16)
Bobcat	Elevation	0.26 (-1.17, 1.62)	Jackrabbit	Elevation	4 (2.24, 5.81)
Bobcat	Canopy	1.67 (-0.06, 3.24)	Jackrabbit	Canopy	-1.35 (-2.68, 0.08)
Bobcat	Burned	0.49 (-1.81, 2.89)	Jackrabbit	Burned	1.19 (-1.31, 3.65)
Bobcat	Burn Lag1	0 (-2.99, 2.96)	Jackrabbit	Burn Lag1	0.04 (-2.14, 2.2)
Bobcat	Burn Lag2	0.52 (-2.06, 3.46)	Jackrabbit	Burn Lag2	2.49 (0.34, 4.58)
Bobcat	Burned X Canopy	0.96 (-1.63, 3.47)	Jackrabbit	Burned X Canopy	-0.14 (-2.74, 2.7)
Bobcat	Burn Lag1 X Canopy	0.61 (-2.57, 3.83)	Jackrabbit	Burn Lag1 X Canopy	0.82 (-1.4, 2.93)
Bobcat	Burn Lag2 X Canopy	-0.73 (-3.17, 2.11)	Jackrabbit	Burn Lag2 X Canopy	1.01 (-1.19, 3.15)
Coyote	Intercept	0.74 (-0.06, 1.45)	Mountain Lion	Intercept	-2.3 (-4.56, -0.13)
Coyote	Ruggedness	0.8 (0.27, 1.33)	Mountain Lion	Ruggedness	0.03 (-1.7, 1.73)
Coyote	Elevation	-0.22 (-0.79, 0.36)	Mountain Lion	Elevation	2.25 (0.58, 3.93)
Coyote	Canopy	-0.23 (-0.82, 0.37)	Mountain Lion	Canopy	1.79 (-0.06, 3.66)
Coyote	Burned	1.78 (0.08, 3.67)	Mountain Lion	Burned	-0.1 (-3.43, 2.8)
Coyote	Burn Lag1	0.73 (-1.36, 2.79)	Mountain Lion	Burn Lag1	-0.77 (-4.62, 2.95)
Coyote	Burn Lag2	0.53 (-1.47, 2.22)	Mountain Lion	Burn Lag2	-1.43 (-5.16, 1.94)
Coyote	Burned X Canopy	1.69 (-0.09, 3.45)	Mountain Lion	Burned X Canopy	1.37 (-2.06, 4.67)
Coyote	Burn Lag1 X Canopy	-0.17 (-2.33, 2.22)	Mountain Lion	Burn Lag1 X Canopy	0.05 (-3.61, 3.6)
Coyote	Burn Lag2 X Canopy	-0.64 (-2.19, 0.9)	Mountain Lion	Burn Lag2 X Canopy	-1.2 (-4.13, 1.83)
Deer	Intercept	5.52 (3.8, 7.09)	Wild Boar	Intercept	-3.39 (-4.59, -2.18)
Deer	Ruggedness	0.33 (-0.77, 1.47)	Wild Boar	Ruggedness	0.98 (0.05, 1.88)
Deer	Elevation	0.45 (-0.88, 1.68)	Wild Boar	Elevation	0.2 (-0.87, 1.33)
Deer	Canopy	1.43 (-0.29, 2.97)	Wild Boar	Canopy	-0.82 (-1.84, 0.2)
Deer	Burned	-0.38 (-2.94, 2.27)	Wild Boar	Burned	-1.66 (-4.76, 1.4)
Deer	Burn Lag1	1.4 (-1.56, 4.41)	Wild Boar	Burn Lag1	-0.05 (-2.71, 2.6)
Deer	Burn Lag2	1.46 (-1.51, 4.49)	Wild Boar	Burn Lag2	-1.77 (-4.9, 1.4)

Deer	Burned X Canopy	1.47 (-1.16, 4.21)	Wild Boar	Burned X Canopy	0.98 (-2.35, 3.84)
Deer	Burn Lag1 X Canopy	-1.02 (-4.09, 2.1)	Wild Boar	Burn Lag1 X Canopy	2.87 (0.21, 5.28)
Deer	Burn Lag2 X Canopy	-0.97 (-3.93, 2.03)	Wild Boar	Burn Lag2 X Canopy	0.71 (-2.28, 3.62)
Fox	Intercept	0.71 (-0.19, 1.64)	Raccoon	Intercept	-0.52 (-1.85, 0.83)
Fox	Ruggedness	0.15 (-0.67, 1.02)	Raccoon	Ruggedness	0.34 (-0.98, 1.6)
Fox	Elevation	0.48 (-0.42, 1.34)	Raccoon	Elevation	-0.89 (-2.28, 0.47)
Fox	Canopy	0.03 (-0.7, 0.77)	Raccoon	Canopy	-0.52 (-1.64, 0.75)
Fox	Burned	0.67 (-1.21, 2.54)	Raccoon	Burned	2.18 (-0.29, 4.66)
Fox	Burn Lag1	0.01 (-1.94, 1.81)	Raccoon	Burn Lag1	-0.6 (-3.41, 2.27)
Fox	Burn Lag2	0.24 (-1.63, 2.06)	Raccoon	Burn Lag2	2.03 (-0.27, 4.54)
Fox	Burned X Canopy	0.68 (-1.37, 2.57)	Raccoon	Burned X Canopy	0.22 (-2.42, 2.91)
Fox	Burn Lag1 X Canopy	2.26 (0.25, 4.39)	Raccoon	Burn Lag1 X Canopy	-1.47 (-4.27, 1.1)
Fox	Burn Lag2 X Canopy	0.03 (-1.63, 1.88)	Raccoon	Burn Lag2 X Canopy	0.11 (-1.85, 2.07)
Gray Squirrel	Intercept	-1.43 (-2.98, 0.15)	Skunk	Intercept	1.37 (-0.8, 3.63)
Gray Squirrel	Ruggedness	-0.97 (-2.55, 0.72)	Skunk	Ruggedness	0.14 (-1.93, 2.27)
Gray Squirrel	Elevation	-1.23 (-2.81, 0.38)	Skunk	Elevation	-0.28 (-2.44, 1.57)
Gray Squirrel	Canopy	0.9 (-0.2, 2.04)	Skunk	Canopy	-0.21 (-2.2, 1.71)
Gray Squirrel	Burned	0.28 (-1.82, 2.75)	Skunk	Burned	1.84 (-1.3, 4.95)
Gray Squirrel	Burn Lag1	0.64 (-1.55, 2.83)	Skunk	Burn Lag1	0.23 (-2.78, 3.15)
Gray Squirrel	Burn Lag2	-0.47 (-3.33, 2.25)	Skunk	Burn Lag2	-0.03 (-3.17, 3.32)
Gray Squirrel	Burned X Canopy	1.01 (-1.32, 3.48)	Skunk	Burned X Canopy	-1.73 (-4.96, 1.32)
Gray Squirrel	Burn Lag1 X Canopy	2.08 (-0.13, 4.47)	Skunk	Burn Lag1 X Canopy	1.37 (-1.45, 4.51)
Gray Squirrel	Burn Lag2 X Canopy	-1.3 (-3.64, 1.37)	Skunk	Burn Lag2 X Canopy	-0.02 (-3.18, 3.21)

899

900 Table S1.3 – Coefficients for occupancy covariates for each single species Occupancy Model.

901 Coefficient estimates, as well as upper and lower credible intervals, are listed for each covariate
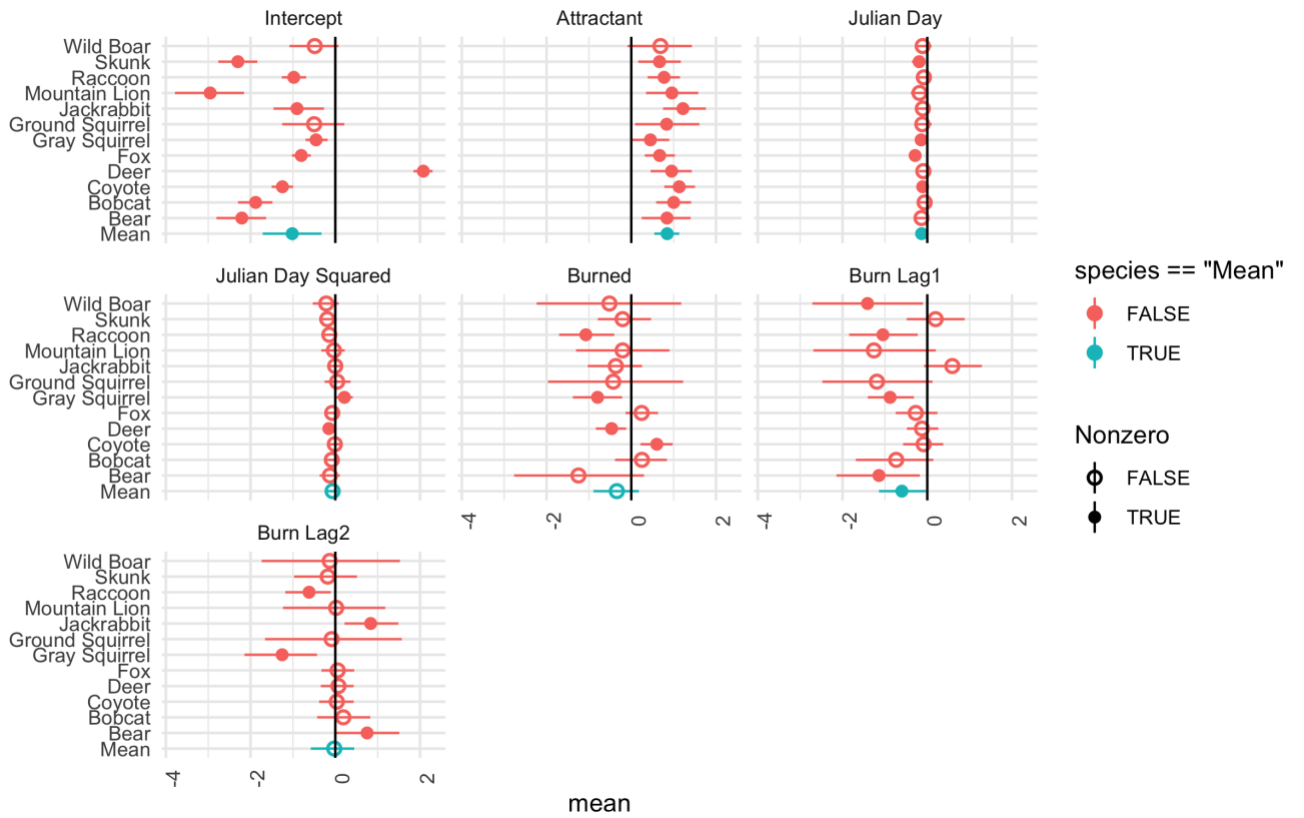
902 and for each species.

903
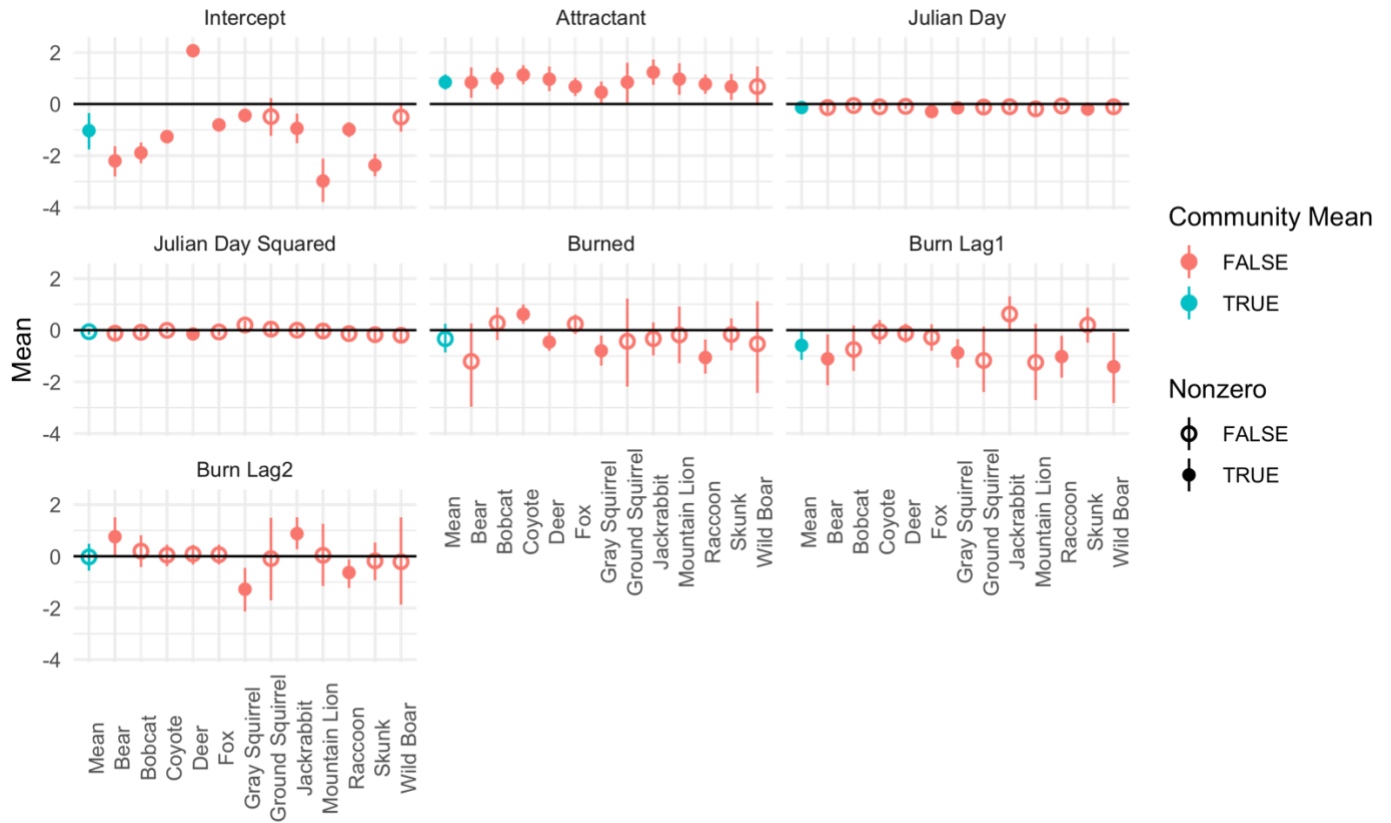
904
905
906 Figure S1.5 – Plotted coefficients of all detection covariates for multi-species occupancy model

907 (MSOM). Both species-specific coefficients and community mean coefficients are included for

908 each covariate.

909

910
911
912 Figure S1.6 - Coefficients of all occupancy covariates for multi-species occupancy model

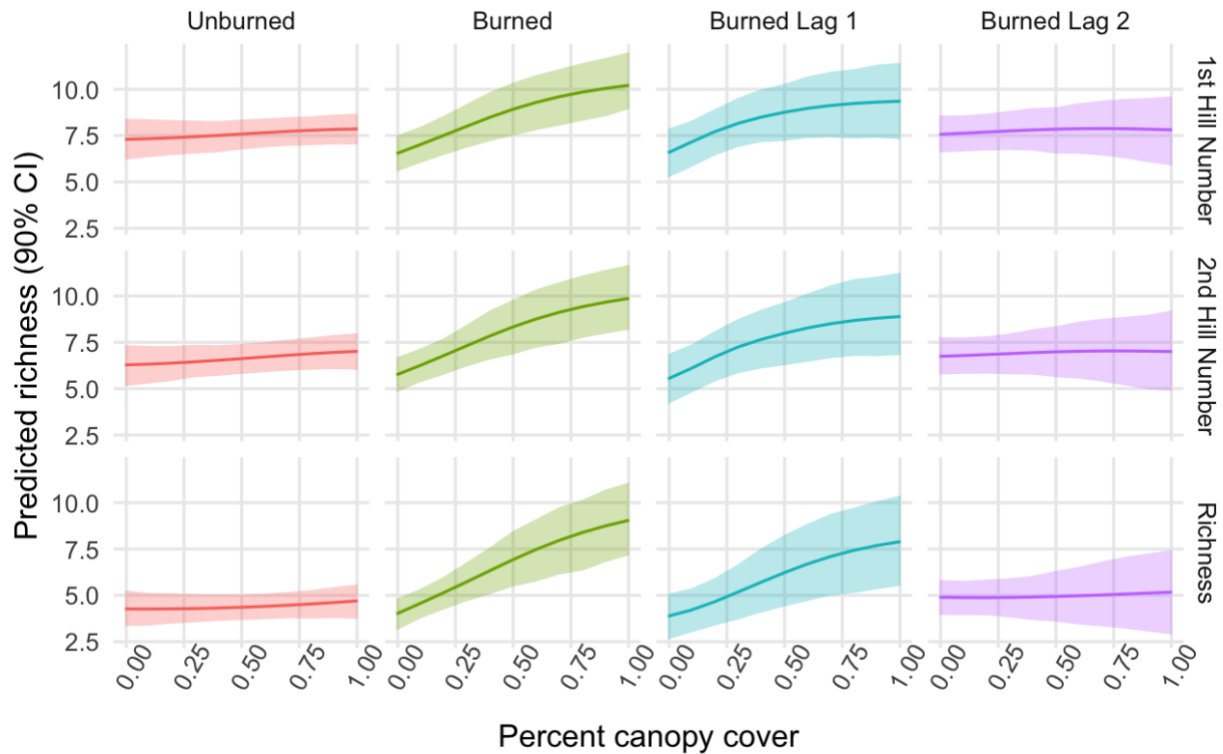913 (MSOM). Both species-specific coefficients and community mean coefficients are included for

914 each covariate.

915
916
917
918
919
920
921
922
923
924
925
926
927
928
929
930

931
932
933   Figure S1.7 - Community richness and Hill number estimates from the multi-species occupancy

934   model (MSOM) across burn histories and canopy cover. All other detection covariates were set

935   to their mean values.

936
937   Literature Cited

938
939   Keeley, J. (2009). Fire intensity, fire severity and burn severity: a brief review and suggested

940   usage. *International journal of wildland fire*, *18*(1), 116-126.

941   Sentinel Hub (2021). Modified Copernicus Sentinel Data. https://www.sentinel-hub.com

942
943
944
945
946
947
948
949
950

951   Authors: Kendall L. Calhoun, Benjamin R. Goldstein, Kaitlyn M. Gaynor, Alex McInturff,

952   Leonel Solorio, Justin S. Brashares

953   Title: Mammalian resilience to megafire in western U.S. woodland savannas

954   Journal Name: Ecological Applications

955

956   **Supplement 2 – Canopy Cover Classification Methods**

957

Data	Source	Projected Coordinate System	Description
Planet Imagery	Planet Labs	WGS 1984 UTM Zone 10N	3m resolution, 4 bands, collected from the month of October from years 2016-2020
Sentinel Imagery	Sentinel Hub	WGS 1984 UTM Zone 10N	20m resolution, 3 bands, collected from the month of October from years 2016-2020
HREC Boundary	Hopland Research and Extension Center	WGS 1984 UTM Zone 10N	Shapefile, used to clip imagery before classification

958

959   Table S2.1 - Canopy Cover Imagery Description Table

960

961   We estimated canopy cover using 20-meter resolution imagery from Sentinel hub

962   (Sentinel Hub, 2021) to create canopy rasters via object-based and supervised classification in

963   ArcGIS Pro (ESRI, 2011) for each year (2016-2020) (Tilahun & Teferie, 2015; Sunde et al.,

964   2020). For this analysis, we categorized imagery d as either 'Covered', which included trees,

965   shrubbery, and other similar vegetation, or 'Uncovered', which included grass, bare ground/soil,

966   and burnt vegetation. We collected satellite imagery from the month of October from each

967   respective year before the start of annual rainfall so grass and bare ground would not look similar

968   to other vegetation. We verified the classified layers using higher resolution imagery obtained

969   from Planet Labs (3m resolution) (Planet Team, 2017) from which we could visually confirm

970   canopy status. For each raster, fifty accuracy assessment points were created and were visually

971   compared to the higher resolution Planet Labs Imagery. Confusion matrices were computed

972   based on the accuracy assessment points to produce overall accuracies for each raster. This

973   supervised classification process was repeated until each raster had an overall accuracy of 80%

974   or higher. Canopy cover values were extracted from a 100m buffer around each camera site for

975   each year to calculate percent canopy cover within the buffered radius.

976

977   Canopy Cover Layers' Accuracy

Year	Accuracy
2016	86%
2017	88%

2018	84%
2019	80%
2020	82%

978

979   Table S2.2 - Canopy cover classification accuracy table. We used object-based image analysis

980   (OBIA) to classify Sentinel Hub Imagery (20m resolution) from Hopland into "Canopy" or "No

981   Canopy" raster layers. Imagery was collected for each year of the study (2016-2020) during the

982   month of October. We created a confusion matrix of 50 randomly generated points across the

983   annual canopy cover rasters and compared canopy classification with the finer scale resolution

984   Planet Labs imagery (3m resolution). We used the finer scale Planet Labs imagery to visually

985   assess the accuracy of each raster layer. Raster layers that had 80% or higher accuracy were

986   accepted and used to calculate % canopy cover covariate for analyses.

987

988   Literature Cited

989

990   ESRI 2011. ArcGIS Desktop: Release 10. Redlands, CA: Environmental Systems Research

991   Institute.

992   Planet Team (2017). Planet Application Program Interface: In Space for Life on Earth. San

993   Francisco, CA. https://api.planet.com.

994   Sentinel Hub (2021). Modified Copernicus Sentinel Data. https://www.sentinel-hub.com

995   Sunde, M. G., Diamond, D. D., Elliott, L. F., Hanberry, P., & True, D. (2020). Mapping high-

996   resolution percentage canopy cover using a multi-sensor approach. Remote Sensing of

997   Environment, 242, 111748. https://doi.org/10.1016/j.rse.2020.111748

998   Tilahun, A., & Teferie, B. (2015). Accuracy assessment of land use land cover classification

999   using Google Earth. *American Journal of Environmental Protection*, *4*(4), 193-198.

1000

1001

1002

1003

1004

1005

1006

1007

1008

1009

1010

1011

1012

1013

1014

1015

1016

1017   Authors: Kendall L. Calhoun, Benjamin R. Goldstein, Kaitlyn M. Gaynor, Alex McInturff,

1018   Leonel Solorio, Justin S. Brashares

1021

1022   Supplement 3 - Multi Species Occupancy Model Equations

1023

1024   The MSOM is defined equivalently to the single-species model with the addition of an

1025   index k denoting that parameters vary between species:

1026

1027 $\text{logit}(\psi_{i,k}) = A0_k + A1_k \times \text{Ruggedness}_i + A2_k \times \text{Elevation}_j + A3_k \times \text{Canopy}_i +$

1028 $A4_k \times \text{Burn History Category}_i + A5_k \times \text{Canopy}_i \times \text{Burn History Category}_i +$

1029 $\text{Site Random Effect}_{i,k}$

1030 $\text{logit}(p_{i,j,k}) = B0_k + B1_k \times \text{Attractant}_i + B2_k \times \text{Julian Day}_{i,j} +$

1031 $B3_k \times \text{Julian Day}^2_{i,j} + B4_k \times \text{Burn History Category}_j$

1032 $z_i \sim \text{Bernoulli}(\psi_{i,k})$

1033 $y_{i,j} \sim \text{Bernoulli}(p_{i,j,k}z_{i,k})$

1034 $\text{Site Random Effect}_{i,k} \sim \text{Normal}(0, \sigma_k)$

1035

1036   with the addition of hyperparameter distributions on A and B defined as:

1037 $Ax_k \sim \text{Normal}(Ax_\mu, \sigma_{Ax})$ for x in 0…5 and k in 0…12

1038 $Bx_k \sim \text{Normal}(Bx_\mu, \sigma_{Ax})$ for x in 0…4 and k in 0…12

1039

1040   where hyperparameters Ax_μ, σ_{Ax} and Bx_μ, σ_{Ax} encode the assumption that species' covariates

1041   follow a normal distribution with a community mean and standard deviation.

1042

1043

1044

1045

1046

1047

1048

1049

1050

1051

1052

1053

1054

1055

1056

1057

1058

1059

1060

1061

1062

1063 Authors: Kendall L. Calhoun, Benjamin R. Goldstein, Kaitlyn M. Gaynor, Alex McInturff,

1064 Leonel Solorio, Justin S. Brashares

1065 Title: Mammalian resilience to megafire in western U.S. woodland savannas

1067

Supplement 4 – Burn History Parameterization

1069

1070 For the burn history categorical variable, we considered four different parameterizations: (1) no

1071 effect of fire, and therefore no parameters; (2) a single effect of "burn" associated with the site-

1072 years following the fire; (3) two postfire levels, "proximate burn" and "lag burn", associated with

1073 burned sites immediately following the fire and in subsequent years, respectively; and (4) three

1074 levels, "proximate burn". These four parameterizations were designed to estimate the effect of

1075 fire on occupancy during and after the fire, while allowing further change postfire if supported

1076 by the data. In all models, we assigned a reference level of "unburned" to all sites pre-burn as

1077 well as unburned sites after the fire. To select a most parsimonious model, we fit the full multi

1078 species occupancy model using each of the above parameterizations and compared their

1079 Watanabe-Akaike information criterion (WAIC) values (Gelman et al., 2014). These

1080 parameterizations were always included in the occupancy and detection sub-models, and in the

1081 occupancy sub-model were interacted with canopy to serve as a proxy for burn severity (with

1082 high-canopy post-burn sites indicating a less comprehensive burn event at that site). Because

1083 WAIC is not a hypothesis test (i.e. a selected model does not indicate that all included variables

1084 are "important" or part of the data-generating process) we did not feel the need to choose models

1085   separately for all species; rather, we investigated posterior estimates of single-species

1086   coefficients on occupancy to understand whether fire categories differed by species.

1087

1088

Parameterization	Pre-fire and unburned sites	Burned sites (2018)	Burned sites (2019)	Burned sites (2020)
(1)	None	None	None	None
(2)	Unburned	Burned	Burned	Burned
(3)	Unburned	Proximate Burned	Lag Burned	Lag Burned
(4)	Unburned	Proximate Burned	Lag Burned 1	Lag Burned 2

1089

1090   Table S4.1 - Schematic of four parameterizations of the "burn history" effect. Sites before the

1091   fire and unburned sites characterize wildlife populations in the absence of proximate fire. After

1092   the fire in the summer of 2018, we group sites affected by the fire into 1-3 categories. We also

1093   consider a null parameterization. We selected between these four parameterizations with WAIC.

1094

1095   Burn History Parameterization Selection Results

1096

1097 Four multi-species occupancy model parameterizations of the effect of fire were compared by

1098 WAIC. The two models with the lowest WAIC values were (3) and (4), those that separated the

1099 lagged effects of burn from the sampling season immediately following the fire event. These two

1100 models were effectively equivalent by WAIC (dWAIC = 0 and 0.715, respectively) but were

1101 decisively selected over models (1) and (2) (WAIC = 44.380 and 9.823, respectively). We

1102 proceeded with analyzing model (4), including effects of "proximate burn," "Burn Lag1," and

1103 "Burn Lag2," as it was highly competitive with (3) and provided better resolution for

1104 understanding the effect of fire on the system over time.

1105

1106

1107 Literature Cited

1108

1109 Gelman, A., Hwang, J., & Vehtari, A. (2014). Understanding predictive information criteria for

1110   Bayesian models. Statistics and Computing, 24(6), 997–1016.

1111   https://doi.org/10.1007/s11222-013-9416-2

1112

1113

1114

1115